January, 1995

LIDS- P 2282

Research Supported By:

ARO DAAL03-92-G-0115
AFOSR F49620-92-J-2002
NSF MIP-9015281

Sensor Array Signal Processing: Two Decades Later*

Krim, H.
Viberg, M.

LIDS-P-2282
January 1995

Sensor Array Signal Processing: Two Decades Later

HAMID KRIM*
Stochastic Systems Group
Massachussets Institute of Technology
Cambridge, MA 02139

MATS VIBERG
Department of Applied Electronics
Chalmers University of Technology
S-412 96 Gothenburg, Sweden

January 11, 1995

Abstract

The problem of estimating the parameters of superimposed signals using an array of sensors has received considerable research interest in the last two decades. Many theoretical studies have been carried out and deep insight has been gained. Traditional applications of array processing include source localization and interference suppression in radar and sonar. The proliferation of estimation algorithms has, however, recently spurred an increasing interest in new applications, such as spatial diversity in personal communications, medical applications and line detection in images.

The goal of this manuscript is to provide a brief review of the recent research activities in sensor array signal processing. The focus is on estimation algorithms. These are classified into spectral-based and parametric methods respectively, depending on the way the estimates are computed. Some of the most well-known algorithms are presented, and their relative merits and shortcomings are described. References to more detailed analyses and special research topics are also given. Some applications of sensor array processing methods are also commented upon, and potential new ones are mentioned. The results of real data experiments are also presented, demonstrating the usefulness of recently proposed estimation techniques.

*The work of the first and last authors was supported in part by the Army Research Office (DAAL-03-92-G-115), Air Force Office of Scientific Research (F49620-92-J-2002) and National Science Foundation (MIP-9015281). The second author is supported by AFOSR grant F49620-93-1-0102 and ONR grant N00014-91-J-1967

1 Introduction

Estimation problems in theoretical as well as applied statistics have long been of great research interest given their ubiquitous presence in a great variety of applications. Parameter estimation has particularly been an area of focus by applied statiticians and engineers as problems required ever improving performance [7, 9, 8]. Many techniques were the result of an attempt of researchers to go beyond the classical Fourier-limit.

As applications expanded, the interest in accurately estimating relevant temporal as well as spatial parameters grew. Sensor array signal processing emerged as an active area of research and was centered on the ability to *fuse* data from several sensors in order to carry out a given estimation task. This framework, as will be described in more detail below, uses to advantage prior information on the data acquisition system (i.e., array geometry, sensor characteristics, etc.). The methods have proven useful for solving several real-world problems, perhaps most notably source localization in radar and sonar. Other more recent applications are discussed in later sections.

Spatial filtering [6, 42] and classical time delay estimation techniques [8] figure among the first approaches to carry out a space-time processing of data sampled at an array of sensors. Both of these approaches were essentially based on the Fourier transform and had inherent limitations. In particular, their ability to resolve closely spaced signal sources is determined by the physical size of the array (the aperture), regardless of the available data collection time and signal-to-noise ratio (SNR). From a statistical point of view, the classical techniques can be seen as spatial extensions of spectral Wiener filtering [129] (or *matched filtering*).

The extension of the time-delay estimation methods to more than one signal[1] and the poor resolution of spatial filtering (or Beamformer) together with an increasing number of novel applications, renewed interest of researchers in statistical signal processing. Its reemergence as an active area of research coincided with the introduction of the well known *Maximum Entropy* (ME) spectral estimation method in geophysics by Burg [21]. This inspired much of the subsequent efforts in spectral estimation, and was intuitively appealing as it was reminiscent of the then long-known Yule-Walker autoregressive estimation model. This similarity was in spite of the fundamental difference with the latter, which uses estimated covariances, whereas the ME method assumes exact knowledge of the auto-covariance function at a limited number of lags. The improvement of the ME technique resulted from making minimal assumptions about the auto-covariance function at lags outside those which are known. Inspired by the laws of physics, Burg proposed to maximize the entropy of the remaining unknown covariance lags. This improved estimation technique, which is readily extended to array processing applications, has been the topic of study in many different fields, see e.g. [9]. With the introduction of subspace-based techniques [91, 12], the research activities accelerated even further. The subspace-based approach relies on geometrical properties of the assumed data model, resulting in a resolution capability which (in theory) is not limited by the array aperture, provided the data collection time and/or SNR are sufficiently large.

[1] These techniques originally used only two sensors.

The quintessential goal of sensor array signal processing is to couple temporal and spatial information, captured by sampling a wavefield with a set of judiciously placed antenna sensors. The wavefield is assumed to be generated by a finite number of emitters, and contains information about signal parameters characterizing the emitters. Given the great number of existing applications for which the above problem formulation is relevant, and the number of newly emerging ones, we feel that a review of the area with more hindsight and perspective provided by time, is in order. The focus is on estimation methods, and many relevant problems are only briefly mentioned. The manuscript is clearly not meant to be exhaustive, but rather as a broad review of the area, and more importantly as a guide for a first time exposure to an interested reader. For more extended treatments , the reader is referred to textbooks such as [30, 88, 52, 48].

The balance of this paper consists of the background material and of the basic problem formulation in Section 2. In Section 3, we introduce spectral-based algorithmic solutions to the signal parameter estimation problem. We constrast these suboptimal solutions to parametric methods in Section 4. Techniques derived from maximum likelihood principles as well as geometric arguments are covered. In Section 5, a number of more specialized research topics are briefly reviewed. In Section 6, a number of real-world problems for which sensor array processing methods have been applied are discussed. Section 7 contains a real data example involving closely spaced emitters and highly correlated signals.

2 Background and Formulation

This section presents the data model assumed throughout this paper, starting from first principles in physics. We also introduce some statistical assumptions and review basic geometrical properties of the model.

2.1 Wave Propagation

Many physical phenomena are either a result of waves propagating through a medium (displacement of molecules) or exhibit a wave-like physical manifestation. A wave propagation may take various forms, depending on the phenomenon and on the medium. In any case, the wave equation has to be satisfied. Our main interest, here, lies in the propagation of electromagnetic waves, which is clearly exposed through a solution of Maxwell's equations,

$$\begin{aligned} \nabla \mathbf{D} &= \rho && (1)\\ \nabla \mathbf{B} &= 0 && (2)\\ \nabla \mathbf{E} &= -\frac{\partial \mathbf{B}}{\partial t} && (3)\\ \nabla \times \mathbf{H} &= \mathbf{J} + \frac{\partial \mathbf{D}}{\partial t}, && (4) \end{aligned}$$

where $\mathbf{D}$, $\mathbf{B}$, $\mathbf{E}$, $\mathbf{H}$, $\mathbf{J}$ respectively denote the electric charge displacement, the magnetic induction, the electric field, the magnetic field and the current density. Equations (1)–(2) express the fact that charges are the sources of electric flux and that there exist no magnetic charges. The last two equations on the other hand, confirm that a time-varying magnetic flux induces a circulation of an electric field and that either a current or a displacement current causes a circulation of a magnetic field.

Using the conservation of rate of change of charge within a volume V_0,

$$\frac{\partial}{\partial t}\int_{V_0} \rho d^3\mathbf{r} = \int \mathbf{J}\cdot\mathbf{n}d\mathbf{S},$$

with $\mathbf{n}$ denoting a surface normal, together with a transform of a surface integral into a volume integral,

$$\nabla \times (\nabla \times \mathbf{V}) = \nabla(\nabla \cdot \mathbf{V}) - \nabla^2\mathbf{V},$$

for any vector $\mathbf{V}$, one can derive after some algebra, the fundamental equations of propagation:

$$\begin{aligned} \nabla(\frac{\rho}{\epsilon}) - \nabla^2\mathbf{E} &= -\mu\frac{\partial}{\partial t}(\mathbf{J} + \epsilon\frac{\partial \mathbf{E}}{\partial t}) && (5)\\ -\nabla^2\mathbf{H} + \epsilon\mu\frac{\partial^2 \mathbf{H}}{\partial t}^2 &= \nabla \times \mathbf{J}\,. && (6) \end{aligned}$$

Solving either of these differential equations (with current charge sources as forcing functions) leads to the solution of the other and results in the well-known traveling wave equation,

$$s(t, \mathbf{p}) = s(\boldsymbol{\alpha}^T \mathbf{p} - \omega t),$$

where ω, and $\boldsymbol{\alpha}$ are respectively the *temporal* angular frequency and the *spatial* slowness vector which determines the direction of the wave propagation, and $\mathbf{p}$ is the position vector. The solution for an arbitrary forcing function (i.e. transmitted waveform) is in general obtained as a superposition of single frequencies (narrowband frequencies, e.g. sinusoidals), and often requires a numerical approach. The structure of the above solution clearly indicates that an exponential-type function coincides with such a behavior. The propagating waves we will be focusing on, in this paper, may emanate from sources such as antennae (E-M waves) or acoustic sources (under water SONAR). The traveling wave equation holds for any application of interest to the estimation methods discussed below. The details of radiating antennae, are left to the excellent book by Jordan [53]. It is also clear that homogeneity and time invariance of the fields are assumed throughout.

With little loss of generality[2], we will assume a model of an exponential traveling wave signal,

$$s(t, \mathbf{p}) = s(t - \boldsymbol{\alpha}^T \mathbf{p}) = e^{j(\omega t - \mathbf{k}^T \mathbf{p})}, \tag{7}$$

where $\omega = 2\pi f$ is the temporal frequency and $\mathbf{k} = \boldsymbol{\alpha}/\omega$ is the wave-vector. The length of $\mathbf{k}$ is the spatial frequency (also referred to as the wavenumber), and equals $2\pi\lambda$, with λ being the wavelength of the carrier. In fact, the model we arrive at will be useful also for non-exponential signals, provided their bandwidth is much smaller than the center frequency[3]. This aspect is important, since in many applications the received signals are modulated carriers. It is also possible that the propagation channel introduces slowly time-varying phase-shifts and/or amplitude modulations of the received signal, although the transmitted signal is a pure tone.

Equation (7) above clearly shows that the phase variation of the signal $s(\cdot)$ is temporal as well as spatial (as it travels some distance in space). Since the phase is dependent upon the spatial coordinates, the traveling mode (determined by the radiating source) will ultimately dictate how the spatial phase is accounted for. An isotropic point source, as will be assumed throughout, results in spherical traveling waves, and all the points lying on the surface of a sphere of radius R share a common phase and are referred to as a *wavefront*. This indicates that the distance between the emitters and the receiving antenna array determines whether or not the sphericity of the wave must be taken into account (near field reception, see e.g. [10]). Far-field receiving conditions implies that the radius R of propagation is so large (compared to the physical size of the array) that a flat plane can be considered, resulting in a *plane wave*. Though not necessary, the latter will be our assumed working model for convenience of exposition.

[2]As already noted, wideband signals can always be expressed as a superposition of exponential signals.

[3]More precisely, the narrowband model holds if the inverse bandwidth is much larger than the time it takes for a traveling wave to propagate across the array.

Note that a linear medium implies the validity of the superposition principle, and thus allows for more than one traveling wave. It is clear from (7) that these propagating waveforms carry information on their origin. This information is expressed in terms of certain signal parameters, such as direction-of-arrival (azimuth and elevation), signal polarization, temporal frequency etc., associated with each emitter. These signal parameters play an important role in many applications, some of which are discussed below, and their estimation has been and continues to be a topic of great research interest. Indeed, this problem forms the essence of sensor array signal processing, which is the topic discussed in greater length in the following sections.

2.2 Parametric Data Model

Most modern approaches to signal processing are model-based, in the sense that they rely on certain assumptions made on the observed data. This section describes the model relevant for the present discussion. It is customary to represent a receiving sensor as an isotropic[4] point source at given spatial coordinates $r_i = (y_{x_i},\, y'_{x_i})$, as shown in Fig. 1.

It is also possible to associate to the i^{th} receiving sensor, a spatially variable pattern (i.e. its response depends on the receiving angle), and account for its directional sensitivity.

We will assume that the array is planar and has L sensors, each of which has coordinates $r_i = (y_{x_i}, y'_{x_i})$ and an impulse response[5]

$$h_i(t, \mathbf{p}_i) = a_i(\theta)\delta(t)\delta(\mathbf{p}_i).$$

As noted earlier, the superposition principle holds for M signals impinging on an L-dimensional array. We can thus define an $L \times M$ impulse response matrix $\mathbf{H}(t, \boldsymbol{\theta})$ from the impinging emitter signals with parameters $\boldsymbol{\theta} = [\theta_1, \theta_2, \ldots, \theta_M]$, to the sensor outputs. Under the stated assumptions, the kl:th element of $\mathbf{H}(t, \boldsymbol{\theta})$ takes the form

$$\mathbf{H}_{kl}(t, \boldsymbol{\theta}) = a_k(\theta_l)\delta(t)\delta(\mathbf{p}_k)\ , \quad k = 1, 2, \ldots, L\ , \quad l = 1, 2, \ldots, M\ . \tag{8}$$

It immediately follows that the sensor outputs, denoted $x_k(t)\, i = \{1, 2, \ldots, L\}$, resulting from a convolution operation can be written as,

$$x_k(t) = \sum_{l=1}^{M} a_k(\theta_l) e^{j(\omega_l t - \mathbf{k}_l^T \mathbf{r}_k)}$$

for purely exponential signals and

$$x_k(t) = \sum_{l=1}^{M} a_k(\theta_l) e^{j(\omega t - \mathbf{k}_l^T \mathbf{r}_k)}\, m_l(t) \tag{9}$$

[4]The radiation/receiving pattern of an isotropic sensor is uniform in all spatial directions.

[5]For convenience, we assume that the sensors have no temporal dynamics. A sufficient assumption would be that their transfer functions are flat over the signal bandwidth.

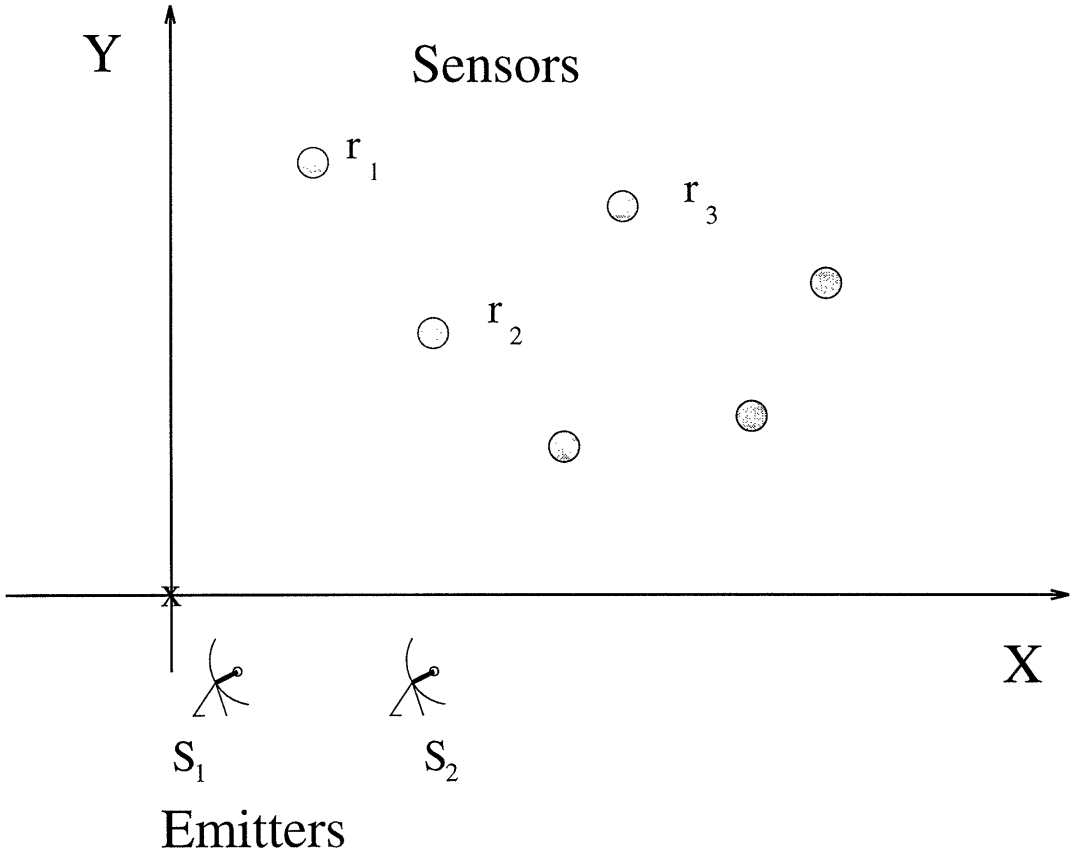

Figure 1: *General two-Dimensional Array*

for narrowband signals. In the latter case, ω is the common center frequency of the signals and $m_l(t)$ represents the complex modulation (gain and phase) of the l:th signal, which by the narrowband assumption is identical at all sensors.

The above equation clearly indicates that the geometry of a given array determines the relative delays of the various arrival angles. This is illustrated for the uniform linear and circular arrays in Figure 2, where it is assumed that the array and the emitters are all in the same plane.

The above formulation can be straightforwardly extended to arrays where additional dimensions provide the flexibility for more signal parameters per source (e.g. azimuth, elevation and polarization). In general, the parameter space can be abstractly represented by some set Θ and may include all of the aforemetioned parameters. However, most of the time we will assume that each θ_l is a real-valued scalar, referred to as the l:th direction-of-arrival (DOA).

The vector representation of the received signal $\mathbf{x}(t)$ is expressed as

$$\mathbf{x}(t) = [\mathbf{a}(\theta_1), \mathbf{a}(\theta_2), \cdots, \mathbf{a}(\theta_M)]\mathbf{s}(t) = \mathbf{A}\mathbf{s}(t), \tag{10}$$

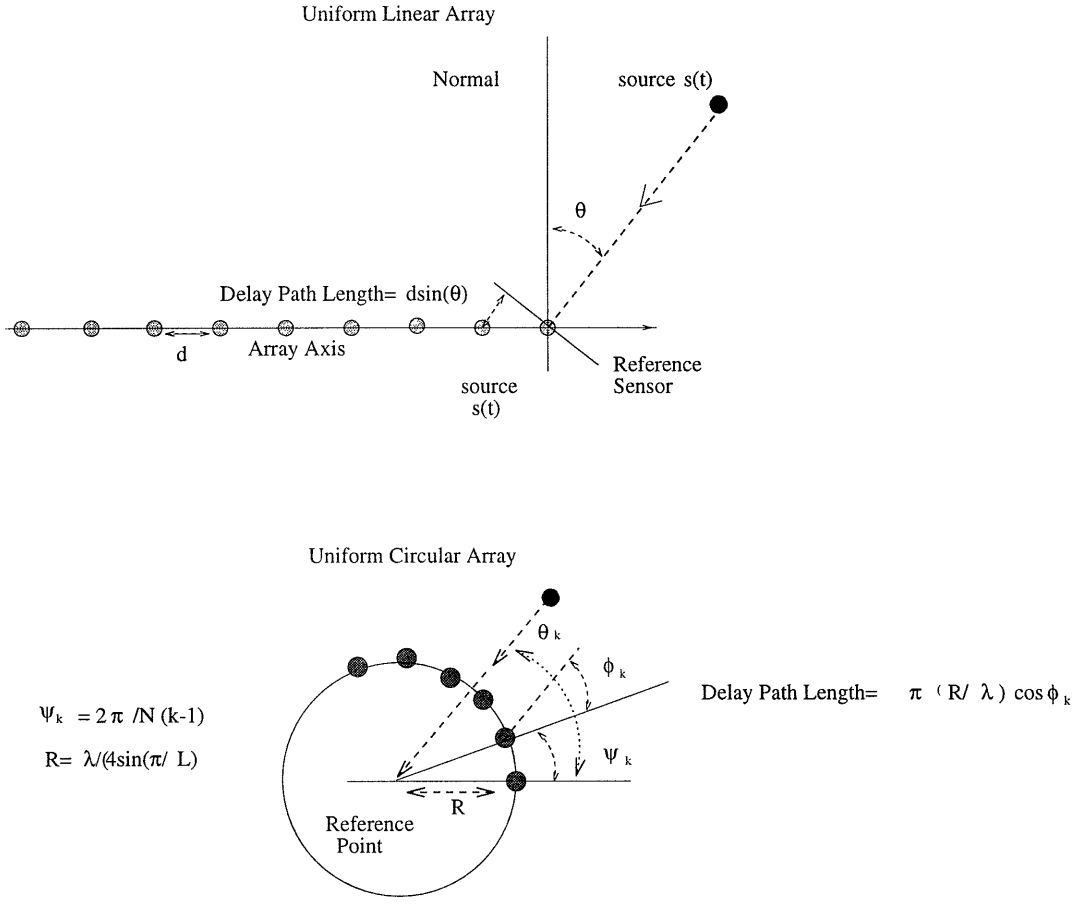

Figure 2: *Common 2-D arrays*

where, with reference to (9),

$$\mathbf{a}(\theta_l) = \left[a_1(\theta_l)e^{j\mathbf{k}_l^T\mathbf{r}_1}, a_2(\theta_l)e^{j\mathbf{k}_l^T\mathbf{r}_2}, \ldots, a_L(\theta_l)e^{j\mathbf{k}_l^T\mathbf{r}_L}\right]^T \tag{11}$$

$$\mathbf{s}(t) = \left[e^{j\omega t}m_1(t), e^{j\omega t}m_2(t), \ldots, e^{j\omega t}m_M(t)\right]^T . \tag{12}$$

The vector $\mathbf{a}(\theta_l)$ is referred to as the l:th array propagation vector, and it describes via $\mathbf{k}_l^T\mathbf{r}_k$ how a plane wave propagates across the array (note that $\mathbf{k}_l$ is a function of the DOA) and via $a_k(\theta_l)$ how the sensors affect the signal amplitude and phase. In many applications, the carrier $e^{j\omega t}$ is removed from the sensor outputs before sampling.

The received signal, will inevitably be corrupted by noise from each of the receiving sensors, giving rise to the following model asssumed throughout,

$$\mathbf{x}(t) = \mathbf{A}\mathbf{s}(t) + \mathbf{n}(t) . \tag{13}$$

The sensor outputs are appropriately sampled at arbitrary time instances, labeled $t = 1, 2, \ldots, N$. Clearly, the process $\mathbf{x}(t)$ can be viewed as a multichannel random process,

whose characteristics can be well understood from its first and second order statistics determined by the underlying signals as well as noise. The sampling frequency is usually much smaller than ω, so that $\mathbf{x}(t)$ often can be regarded as temporally white.

2.3 Assumptions

The signal parameters which are of interest in this paper, are of spatial nature, and thus require the cross-covariance information among the various sensors, i.e. the *spatial covariance* matrix,

$$\mathbf{R} = \mathrm{E}\{\mathbf{x}(t)\mathbf{x}^H(t)\} = \mathbf{A}\mathrm{E}\{\mathbf{s}(t)\mathbf{s}^H(t)\}\mathbf{A}^H + \mathrm{E}\{\mathbf{n}(t)\mathbf{n}^H(t)\} . \tag{14}$$

Here, the symbol $(\cdot)^H$ denotes complex conjugate and transpose (Hermite). Assuming temporal whiteness and denoting $\delta_{t,s}$ the Kronecker delta, the source covariance matrix is defined as

$$\mathrm{E}\{\mathbf{s}(t)\mathbf{s}^H(s)\} = \mathbf{P}\,\delta_{t,s} \tag{15}$$

whereas the noise covariance matrix is modeled as given by

$$\mathrm{E}\{\mathbf{n}(t)\mathbf{n}^H(s)\} = \sigma^2\,\mathbf{I}\,\delta_{t,s} . \tag{16}$$

Thus, it is assumed that the noise have the same level σ^2 in all sensors, and is uncorrelated from sensor to sensor. Such noise is usually termed *spatially white*, and is a reasonable model for e.g. receiver noise. However, other man-made noise sources need not result in spatial whiteness, in which case the noise must be pre-whitened. More specifically, if the noise covariance matrix is $\mathbf{Q}$, the sensor outputs are multiplied by $\mathbf{Q}^{-1/2}$ ($\mathbf{Q}^{1/2}$ denotes a Hermitean square-root factor of $\mathbf{Q}$) prior to further processing. The source covariance matrix, $\mathbf{P}$ is often assumed to be nonsingular (a rank-deficient $\mathbf{P}$, as in the case of temporally coherent signals, is discussed in Sections 3.3 and 4).

In the later development, the spectral factorization of $\mathbf{R}$ will be of central importance, and its positivity guarantees the following representation,

$$\mathbf{R} = \mathbf{A}\mathbf{P}\mathbf{A}^H + \sigma^2\mathbf{I} = \mathbf{U}\mathbf{\Lambda}\mathbf{U}^H, \tag{17}$$

with $\mathbf{U}$ unitary and $\mathbf{\Lambda} = \mathrm{diag}\{\lambda_1, \lambda_2, \cdots, \lambda_L\}$ a diagonal matrix of real and positive eigenvalues, such that $\lambda_1 \geq \lambda_2 \geq \cdots \geq \lambda_L$. Observe that any vector orthogonal to $\mathbf{A}$ is an eigenvector of $\mathbf{R}$ with the eigenvalue σ^2. There are $L - M$ linearly independent such vectors. Since the remaining eigenvalues are all larger than σ^2, we can split the eigenvalue/vector pairs into noise eigenvectors (corresponding to eigenvalues $\lambda_{M+1} = \cdots = \lambda_L = \sigma^2$) and signal eigenvectors (corresponding to eigenvalues $\lambda_1 \geq \cdots \geq \lambda_M > \sigma^2$). This results in the representation

$$\mathbf{R} = \mathbf{U}_s\mathbf{\Lambda}_s\mathbf{U}_s^H + \mathbf{U}_n\mathbf{\Lambda}_n\mathbf{U}_n^H , \tag{18}$$

where the columns of the signal subspace matrix $\mathbf{U}_s$ are the M principal eigenvectors, and the noise subspace matrix $\mathbf{U}_n$ contains the eigenvectors corresponding to the multiple eigenvalue σ^2, i.e. $\mathbf{\Lambda}_n = \sigma^2\mathbf{I}$. Since all noise eigenvectors are orthogonal to $\mathbf{A}$, the columns

of $\mathbf{U}_s$ must span the range space of $\mathbf{A}$ whereas those of $\mathbf{U}_n$ span its orthogonal complement (the nullspace of $\mathbf{A}^H$). The projection operators onto these signal and noise subspaces are defined as

$$\begin{aligned} \mathbf{\Pi} &= \mathbf{U}_s\mathbf{U}_s^H = \mathbf{A}(\mathbf{A}^H\mathbf{A})^{-1}\mathbf{A}^H \\ \mathbf{\Pi}^\perp &= \mathbf{U}_n\mathbf{U}_n^H = \mathbf{I} - \mathbf{A}(\mathbf{A}^H\mathbf{A})^{-1}\mathbf{A}^H \ , \end{aligned} \tag{19}$$

which clearly satisfy

$$\mathbf{I} = \mathbf{\Pi} + \mathbf{\Pi}^\perp. \tag{20}$$

2.4 Problem Definition

The problem of central interest herein is that of estimating the DOAs of emitter signals impinging on a receiving array, when given a finite data set $\{\mathbf{x}(t)\}$ observed over $\{t = 1, 2, \ldots, N\}$. As noted earlier, we will primarily focus on reviewing a number of techniques based on second-order statistics of data.

All of the earlier formulation assumed the existence of exact quantities, i.e. infinite observation time. It is clear that in practice sample estimates are only possible and are designated by a^. The ML estimate of $\mathbf{R}$ is given by[6],

$$\widehat{\mathbf{R}} = \frac{1}{N}\sum_{t=1}^{N}\mathbf{x}(t)\mathbf{x}^H(t). \tag{21}$$

A corresponding eigen-representation similar to that of $\mathbf{R}$ is defined as

$$\widehat{\mathbf{R}} = \widehat{\mathbf{U}}_s\widehat{\mathbf{\Lambda}}_s\widehat{\mathbf{U}}_s^H + \widehat{\mathbf{U}}_n\widehat{\mathbf{\Lambda}}_n\widehat{\mathbf{U}}_n^H \ . \tag{22}$$

This decomposition will be extensively used in the description and implementation of the subspace-based estimation algorithms. Throughout the paper, the number of underlying signals, M, in the observed process is considered known. There are, however, good and consistent signal enumeration techniques available [124, 93, 29, 61] in the event that such an information is not available, see also Section 5.1.

In Sections 3 and 4, for space reasons, we limit the discussion to the best known estimation techniques, respectively classified as *Spectral-Based* and *Parametric* methods. With the full knowledge of existence of a number of good variations which address particular problems of those described here, the reference list attempts to cover a portion of the gap which clearly can never be filled.

[6]Strictly speaking, (21) does not give the ML estimate of the array covariance matrix, since it does not exploit its parametric structure. See Section 4 for further details on this aspect. The sample covariance matrix (21) is sometimes referred to as an unstructured ML estimate.

3 Spectral-Based Algorithmic Solutions

As pointed out earlier, we classify the parameter estimation techniques into two main categories, namely the *spectral-based* and the *parametric* approaches. In the former, one forms some spectrum-like function of the parameter(s) of interest, e.g. the DOA. The location of the highest (separated) peaks of the function in question are taken as the DOA estimates. The parametric techniques, on the other hand, require a simultaneous search for all parameters of interest. While often more accurate, the latter approach is usually more computationally complex.

The spectral-based methods in turn are divided into the beamforming approaches and the subspace-based methods.

3.1 Beamforming Techniques

The first attempt to automatically localize signal sources using antenna arrays was through beamforming techniques. The idea is to "steer" the array in one direction at the time and measure the output power. The locations of maximum power yield the DOA estimates. The array is steered by forming a linear combination of the sensor outputs

$$y(t) = \sum_{i=1}^{L} w_i^* x_i(t) = \mathbf{w}^H \mathbf{x}(t) \ , \tag{23}$$

where $(\cdot)^*$ denotes complex conjugate. Given samples $y(1), y(2), \ldots, y(N)$, the output power is measured by

$$P(\mathbf{w}) = \frac{1}{N} \sum_{t=1}^{N} |y(t)|^2 = \frac{1}{N} \sum_{t=1}^{N} \mathbf{w}^H \mathbf{x}(t) \mathbf{x}^H(t) \mathbf{w} = \mathbf{w}^H \widehat{\mathbf{R}} \mathbf{w} \tag{24}$$

where $\widehat{\mathbf{R}}$ is defined in (21). Different beamforming approaches correspond to different choices of weighting vector $\mathbf{w}$. For an excellent review of the utility of beamforming methods, we refer to [115].

3.1.1 Conventional Beamformer

Following the development of the *Maximum Entropy* criterion formulated by Burg [21] in spectral analysis, a plethora of estimation algorithms appeared in the literature, each using a different optimization criterion. For a given structured array, the first algorithm which precedes even the entropy-based algorithm, is one which maximizes its output power for a certain input. Suppose we wish to maximize the output power from a certain direction θ. The array output, assuming a signal at θ corrupted by additive noise, is given by

$$\mathbf{x}(t) = \mathbf{a}(\theta) s(t) + \mathbf{n}(t) \ .$$

The problem of maximizing the output power is then formulated as

$$\begin{aligned} \max_{\mathbf{w}} \mathrm{E}\{\mathbf{w}^H \mathbf{x}(t)\mathbf{x}^H(t)\mathbf{w}\} &= \max_{\mathbf{w}} \mathbf{w}^H \mathrm{E}\{\mathbf{x}(t)\mathbf{x}^H(t)\}\mathbf{w} \\ &= \max_{\mathbf{w}} \left\{ \mathrm{E}|s(t)|^2 \left|\mathbf{w}^H \mathbf{a}(\theta)\right|^2 + \sigma^2 |\mathbf{w}|^2 \right\}, \end{aligned} \tag{25}$$

where the assumption of spatially white noise is used in the last equality. Employing a norm constraint on $\mathbf{w}$ to ensure a finite solution, we find that the maximizing weight vector is given by

$$\mathbf{w}_{BF} = \mathbf{a}(\theta). \tag{26}$$

The above weight vector can be interpreted as a spatial filter, which has been matched to the impinging signal. Intuitively, the array weighting equalizes the delays experienced by the signal on various sensors to maximally combine their contributions. Figure 3 illustrates this point.

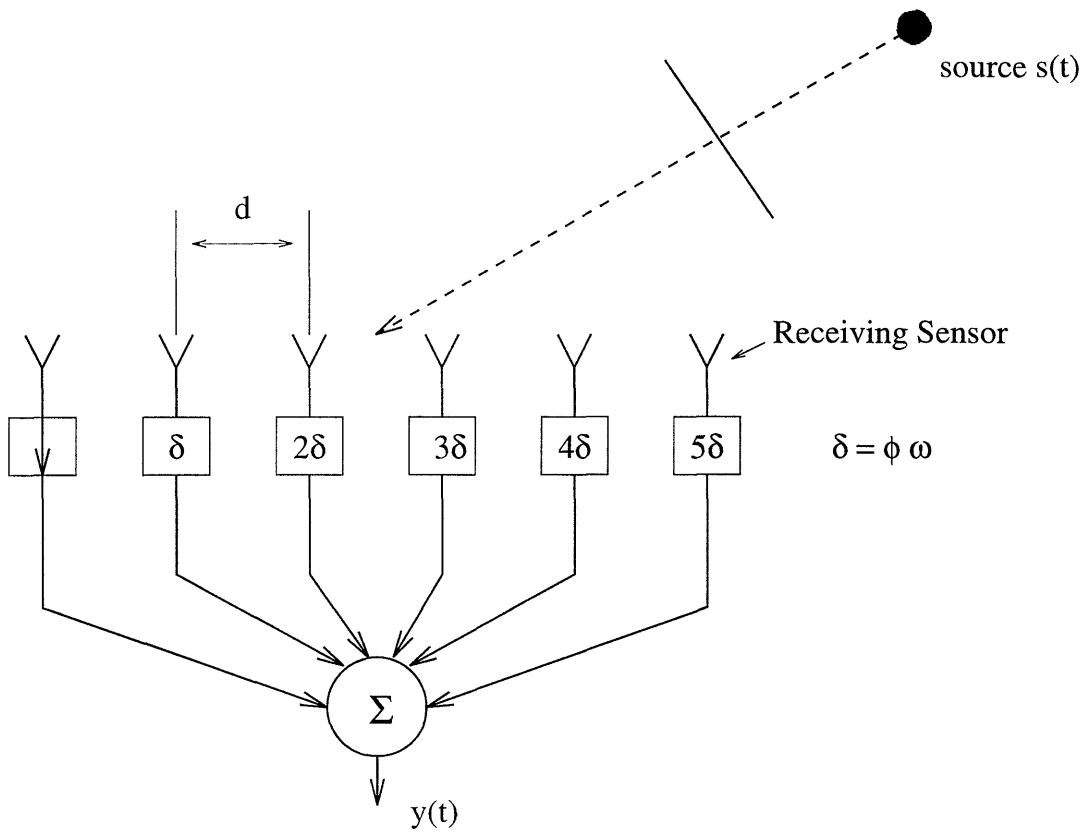

Figure 3: Standard Beamformer

Inserting the weighting vector (26) into (24), the classical *spatial spectrum* is obtained as

$$P_{BF}(\theta) = \mathbf{a}^H(\theta)\widehat{\mathbf{R}}\mathbf{a}(\theta). \tag{27}$$

For a uniform linear array (ULA), the steering vector $\mathbf{a}(\theta)$ takes the form (see Figure 2)

$$\mathbf{a}(\theta) = \left[1, e^{j\phi}, \ldots, e^{j(L-1)\phi}\right]^T , \tag{28}$$

where

$$\phi = -\frac{\omega}{c} d \sin(\theta) \tag{29}$$

is termed the *electrical angle*. Here, ω is the center frequency of the signals, c is the speed of propagation, d is the inter-element separation and the DOA θ is taken relative to the normal of the array. By inserting (28) into (27), we obtain $P_{BF}(\theta)$ as the spatial analogue of the classical periodogram in temporal time series analysis, see e.g. [83]. Unfortunately, the spatial spectrum suffers from the same resolution problem as does the periodogram. The standard beamwidth for a ULA is $\phi_B = 2\pi/L$, and sources whose electrical angles are closer than ϕ_B will not be resolved by the conventional beamformer, regardless of the available data quality.

3.1.2 Capon's Beamformer

In an attempt to alleviate the limitations of the above beamformer, such as its resolving power of two sources spaced closer than a beamwidth, researchers have proposed numerous modifications. A well-known method was proposed by Capon [23], who formulated an algorithm as a dual of the beamformer. The optimization problem was posed as

$$\begin{aligned} & \min_{\mathbf{w}} P \\ \text{subject to} \quad & \mathbf{w}^H \mathbf{a}(\theta) = 1 \, . \end{aligned}$$

Hence, Capon's beamformer attempts to minimize the power received from noise and any signals coming from other directions than θ, while maintaining a fixed gain in the "look direction" θ. The optimal $\mathbf{w}$ can be found using, e.g., the technique of Lagrange multipliers, resulting in

$$\mathbf{w}_{CAP} = \frac{\widehat{\mathbf{R}}^{-1}\mathbf{a}(\theta)}{\mathbf{a}^H(\theta)\widehat{\mathbf{R}}^{-1}\mathbf{a}(\theta)} \, . \tag{30}$$

The above weight in turn leads to the following "spatial spectrum" upon insertion into (24)

$$P_{CAP}(\theta) = \frac{1}{\mathbf{a}^H(\theta)\widehat{\mathbf{R}}^{-1}\mathbf{a}(\theta)} \, . \tag{31}$$

It is easy to see why Capon's beamformer outperforms the more classical one, as the former uses every single degree of freedom to concentrate the received energy along one direction, namely the bearing of interest. The Capon beamformer is allowed to give up some noise suppression capability to provide a focused "nulling" in the directions where there are other sources present. The spectral leakage from closely spaced sources is therefore reduced, though the resolution capability of the Capon beamformer is still dependent upon the array aperture.

A number of alternative methods for beamforming have been proposed, addressing various issues such as partial signal cancelling due to signal coherence [128] and beam shaping and interference control [41, 20, 115].

3.2 Subspace-Based Methods

Many spectral methods in the past, have implicitly called upon the eigen structure of a process to carry out its analysis (e.g. Karhunen-Loève representation). One of the most significant contributions came about when the eigen-structure of a process was explicitly invoked, and its intrinsic properties were directly used to provide a solution to an underlying estimation problem for a given observed process.

Early approaches involving invariant subspaces of observed covariance matrices include principal component factor analysis [49] and errors-in-variables time series analysis [58]. In the engineering literature, Pisarenkos work [81] in time series analysis was among the first to be published. However, the tremendous interest in the subspace approach is mainly the result of the introduction of the MUSIC (Multiple SIgnal Classification) algorithm [91, 12].

3.2.1 The MUSIC Algorithm

As noted in Section 2.3, the structure of the exact covariance matrix together with the spatial white noise assumption implies that its eigendecomposition can be expressed as

$$\mathbf{R} = \mathbf{A}\mathbf{P}\mathbf{A}^H + \sigma^2\mathbf{I} = \mathbf{U}_s\mathbf{\Lambda}_s\mathbf{U}_s^H + \sigma^2\,\mathbf{U}_n\mathbf{U}_n^H\ , \tag{32}$$

where the diagonal matrix $\mathbf{\Lambda}_s$ contains the M largest eigenvalues (assuming $\mathbf{A}\mathbf{P}\mathbf{A}^H$ to be of full rank). Since the eigenvectors in $\mathbf{U}_n$ (the noise eigenvectors) are orthogonal to $\mathbf{A}$, we have

$$\mathbf{U}_n^H\mathbf{a}(\theta) = 0\ , \quad \theta \in \{\theta_1, \ldots, \theta_M\}\ . \tag{33}$$

To allow for unique DOA estimates, the array is usually assumed to be *unambiguous*; that is, any collection of L steering vectors corresponding to distinct DOAs η_k forms a linearly independent set $\{\mathbf{a}(\eta_1), \ldots, \mathbf{a}(\eta_L)\}$. In particular, a ULA can be shown to be unambiguous if the DOAs are confined to $-\pi/2 < \theta < \pi/2$ and $d < \lambda/2$. Under this assumption, $\theta_1, \ldots, \theta_M$ are the only possible solutions to the relation (33), which could therefore be used to locate the DOAs exactly.

In practice, as previously noted, an estimate of the covariance matrix $\widehat{\mathbf{R}}$ is obtained, and its eigenvectors are split into the signal and noise eigenvectors as in (22). The orthogonal projector onto the noise subspace is estimated as

$$\widehat{\mathbf{\Pi}}^{\perp} = \widehat{\mathbf{U}}_n\widehat{\mathbf{U}}_n^H\ . \tag{34}$$

The MUSIC "spatial spectrum" is then defined as

$$P_M(\theta) = \frac{\mathbf{a}^H(\theta)\mathbf{a}(\theta)}{\mathbf{a}^H(\theta)\widehat{\mathbf{\Pi}}^{\perp}\mathbf{a}(\theta)} \tag{35}$$

(the denominator in (35) is included to account for non-uniform sensor gain and phase characteristics). Although $P_M(\theta)$ is not a true spectrum in any sense (it is merely the distance between two subspaces), it exhibits peaks in the vicinity of the true DOAs provided $\widehat{\mathbf{\Pi}}^{\perp}$ is close to $\mathbf{\Pi}^{\perp}$.

The performance improvement of this method was so significant that it became an alternative to most existing estimators. In particular, it follows from the above reasoning that estimates of an arbitrary accuracy can be obtained if the data collection time is sufficiently long or the SNR is adequately high. Thus, in contrast to the beamforming techniques, the MUSIC algorithm provides *statistically consistent* estimates. Though the MUSIC function (35) does not represent a spectral estimate, its important limitation is still the failure to resolve closely spaced signals in small samples and at low SNR. This loss of resolution is more serious for highly correlated signals. In the limiting case of coherent signals[7], the property (33) no longer holds and the method fails to yield consistent estimates, see e.g. [60]. The mitigation of this limitation is an important issue and is separately addressed at the end of this section.

3.2.2 Extensions to MUSIC

The MUSIC algorithm spawned a significant research activity which led to a multitude of proposed modifications. These were attempts to improve/overcome some of its shortcomings in various specific scenarios. The most notable was the unifying theme of *weighted MUSIC* which, for different $\mathbf{W}$, particularized to different algorithms,

$$P_{WM}(\theta) = \frac{\mathbf{a}^H(\theta)\mathbf{a}(\theta)}{\mathbf{a}^H(\theta)\widehat{\mathbf{\Pi}}^{\perp}\mathbf{W}\widehat{\mathbf{\Pi}}^{\perp}\mathbf{a}(\theta)} . \tag{36}$$

The weighting matrix $\mathbf{W}$ is introduced to take into account (if desired) the influence of each of the eigenvectors. It is clear that a uniform weighting of the eigenvectors, i.e. $\mathbf{W} = \mathbf{I}$, results in the original MUSIC method. As shown in [99], this is indeed the optimal weighting in terms of yielding estimates of minimal asymptotic variance. However, in difficult scenarios involving small samples, low SNR and highly correlated signals, a carefully chosen non-uniform weighting may still improve the resolution capability of the estimator (see Section 7).

One particularly useful choice of weighting is given by [62]

$$\mathbf{W} = \mathbf{e}_1\mathbf{e}_1^T , \tag{37}$$

where $\mathbf{e}_1$ is the first column of the $L \times L$ identity matrix. This corresponds to the Min-Norm algorithm, originally proposed by Tufts and Kumaresan [64, 113] for ULAs and extended to arbitrary arrays in [66]. As shown in [55], the Min-Norm algorithm indeed exhibits a lower bias and hence a better resolution than the original MUSIC algorithm.

[7]Two signals are said to be coherent if one is a scaled version of the other.

3.2.3 Resolution-Enhanced Spectral Based Methods

The MUSIC algorithm is known to enjoy a property of high accuracy in estimating the phases of the roots corresponding to DOA of sources. The bias in the estimates radii [62], however, affects the resolution of closely spaced sources when using the spatial spectrum.

A solution first proposed in [13], and later in [37, 19], is to couple the MUSIC algorithm with some spatial prefiltering, to result in what is known as *Beamspace Processing*. This is indeed equivalent to preprocessing the received data with a predefined matrix $\mathbf{T}$, whose columns can be chosen as the steering vectors for a set of chosen directions:

$$\mathbf{z}(t) = \mathbf{T}^H \mathbf{x}(t) \ . \tag{38}$$

Clearly, the steering vectors $\mathbf{a}(\theta)$ are then replaced by $\mathbf{T}^H\mathbf{a}(\theta)$ and the noise covariance for the beamspace data becomes $\sigma^2\,\mathbf{T}^H\mathbf{T}$. For the latter reason, $\mathbf{T}$ is often orthogonalized before application to $\mathbf{x}(t)$.

It is clear that if a certain spatial sector is selected to be swept (e.g. some prior knowledge about the broad direction of arrival of the sources may be available), one can potentially experience some gain, the most obvious being computational, as a smaller dimensionality of the problem usually results. It has, in addition, been shown that the bias of the estimates is decreased when employing MUSIC in beamspace as opposed to the "element space" MUSIC [37, 137]. As expected, the variance of the DOA estimates is not improved, but a certain robustness to spatially correlated noise has been noted in [37]. The latter fact can intuitively be understood when one recalls that the spatial pre-filter has a bandpass character, which will clearly tend to whiten the noise.

Other attempts to improving the resolution of the MUSIC method are presented in e.g. [56, 33, 135], based on different modifications of the criterion function.

3.3 Coherent Signals

Though unlikely that one would deliberately transmit two coherent signals from distinct directions, such a phenomenon is not uncommon as either a natural result of a multipath propagation effect, or intentional unfriendly jamming. The end result is a rank deficiency in the source covariance matrix $\mathbf{P}$. This, in turn, results in a divergence of a signal eigenvector into the noise subspace. Therefore, in general $\mathbf{U}_n^H\mathbf{a}(\theta) \neq 0$ for any θ and the MUSIC "spectrum" may fail to produce peaks at the location of DOAs. In particular, the ability to resolve closely spaced sources is dramatically reduced for highly correlated signals, see. e.g. [63].

In the simple case of two coherent sources being present and a uniform linear array, there is a fairly straightforward way to "de-correlate" the signals. The idea is to employ a forward-backward (FB) averaging as follows. Note that a ULA steering vector (28) remain unchanged, up to a scaling, if its elements are reversed and complex conjugated. More precisely, let $\mathbf{J}$ be an $L \times L$ exchange matrix, whose components are zero excepts for ones on the anti-diagonal. Then, for a ULA it holds that

$$\mathbf{J}\mathbf{a}^*(\theta) = e^{-j(L-1)\phi}\mathbf{a}(\theta) \ . \tag{39}$$

The so-called backward array covariance matrix therefore takes the form

$$\mathbf{R}_B = \mathbf{J}\mathbf{R}^*\mathbf{J} = \mathbf{A}\mathbf{\Phi}^{-(L-1)}\mathbf{P}\mathbf{\Phi}^{-(L-1)}\mathbf{A}^H + \sigma^2\,\mathbf{I}\,, \tag{40}$$

where $\mathbf{\Phi}$ is a diagonal matrix with $e^{j\phi_k}$, $k = 1, \ldots, M$ on the diagonal. By averaging the usual array covariance and $\mathbf{R}_B$, one obtains the FB array covariance

$$\begin{aligned} \mathbf{R}_{FB} &= \frac{1}{2}\left(\mathbf{R} + \mathbf{J}\mathbf{R}^*\mathbf{J}\right) \\ &= \mathbf{A}\widetilde{\mathbf{P}}\mathbf{A}^H + \sigma^2\,\mathbf{I}\,, \end{aligned} \tag{41}$$

where the new "source covariance matrix" $\widetilde{\mathbf{P}} = (\mathbf{P} + \mathbf{\Phi}^{-(L-1)}\mathbf{P}\mathbf{\Phi}^{-(L-1)})/2$ generically has full rank. The FB version of any covariance-based algorithm simply consists of replacing $\widehat{\mathbf{R}}$ with $\widehat{\mathbf{R}}_{FB}$, defined as in (41). Note that this transformation has also been used in noncoherent scenarios, and in particular in time series analysis, for merely improving the variance of the estimates.

In a more general scenario where more than two coherent sources are present, forward-backward averaging cannot restore the rank of the signal covariance matrix on its own. A heuristic solution of this problem was first proposed in [128] for uniform linear arrays, and later formalized and extended[8] in [31, 93]. The idea of the so-called *spatial smoothing* technique is to split the ULA into a number of overlapping subarrays. The steering vectors of the subarrays are assumed to be identical up to different scalings, and the subarray outputs can therefore be averaged before computing the covariance matrix. Similar to (41), the spatial smoothing induces a random phase modulation which in turn decorrelates the signals that caused the rank deficiency. This is pictorially shown in Figure 4.

Formally, the transformation can also be carried out by an averaging procedure of overlapping diagonal submatrices of the original covariance matrix $\mathbf{R}$, and thus as a result, "unfold" the collapsed signal subspace with an appropriate choice of the submatrix size (i.e. subarray size). A compact expression for this smoothed matrix $\widetilde{\mathbf{R}}$ can be written in terms of a filtering matrix $\mathbf{F}$ as follows. If p is a positive integer smaller than L (p is the number of elements in the subarrays), $n_s = L - p + 1$ is the number of subarrays, $\mathbf{F} = [\mathbf{F}_{1p}|\mathbf{F}_{2p}|\cdots|\mathbf{F}_{n_sp}]$, is a $p \times n_s L$ windowing matrix defined by $\mathbf{F}_{ip} = [\mathbf{0}_{p\times(i-1)}|\mathbf{I}_p|\mathbf{0}_{p\times(L-i-p+1)}]$, $i = 1, 2, \cdots, n_s$, then we can write

$$\widetilde{\mathbf{R}} = \mathbf{F}\left(\mathbf{I}_{n_s} \otimes (\mathbf{R})\right)\mathbf{F}^{\mathrm{T}}\,.$$

Here, $\otimes$ denotes the Kronecker matrix product and $\mathbf{I}_{n_s}$ is the $n_s \times n_s$ identity matrix. The rank of the averaged source covariance matrix $\widetilde{\mathbf{P}}$ can be shown to increase by 1 w.p.1 [27] for each additional subarray in the averaging, until it reaches its maximum value M.

The drawback with spatial smoothing is that the effective aperture of the array is reduced, since the subarrays are smaller than the original array. However, despite this loss

[8]The so-called spatial smoothing transformation requires a translational invariance which is valid for ULA. Conceptually, however, one could always map the steering vectors for any array into those of a ULA and proceed with the transformation described here, see further [40].

of aperture, the spatial smoothing transformation mitigates the limitation of all subspace-based estimation techniques while retaining the computational efficiency of the unidimensional spectral searches. As seen in the next section, the parametric techniques, in general do not experience such problems when faced with coherent signals. They require, on the other hand a more complicated multidimensional search. Let us again stress on the fact that spatial smoothing and FB averaging is essentially limited to ULAs. When using more general arrays (e.g. circular), some sort of transformation of the received data to that of a ULA must precede the smoothing transformation. Such a transformation is conceptually possible, but requires in general some *a priori* knowledge of the source locations.

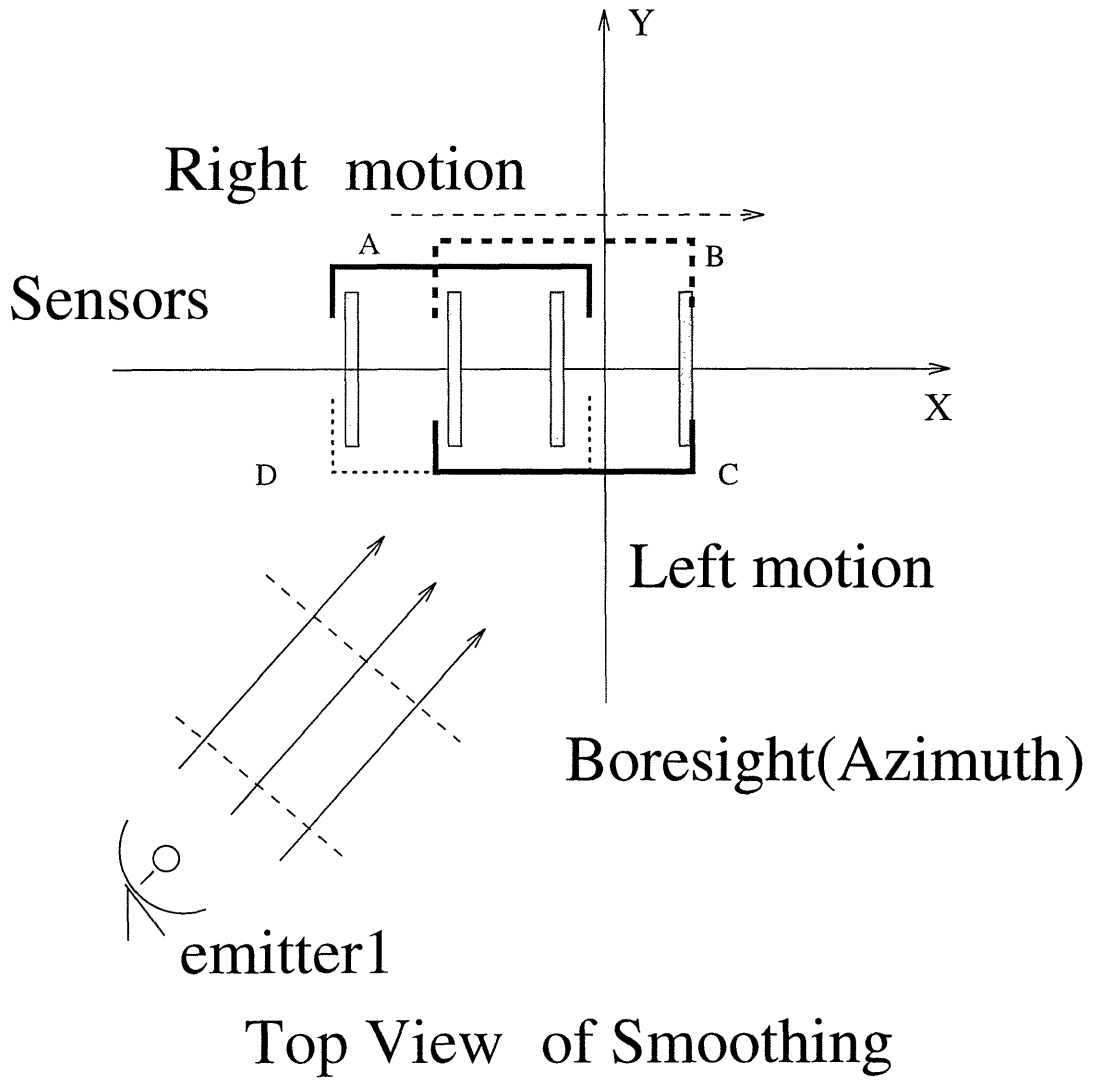

Figure 4: *Smoothing Transformation*

4 Parametric Methods

While the spectral-based methods presented in the previous section are computationally attractive, they do not always yield sufficient accuracy. In particular, for scenarios involving highly correlated (or even coherent) signals, the performance of spectral-based methods may be insufficient. An alternative is to more fully exploit the underlying data model, leading to so-called *parametric* array processing methods. As we shall see, coherent signals impose no conceptual difficulties for such methods. The price to pay for this increased efficiency is that the algorithms typically require a numerical optimization to find the estimates. For uniform linear arrays (ULAs), the search can, however, be avoided with little (if any) loss of performance.

Perhaps the most important model-based approach in signal processing is the maximum likelihood (ML) technique. This methodology requires a statistical framework for the data generation process. Though not necessary, the vast majority of existing ML algorithms assume Gaussian noise. Two different assumptions about the emitter signals have led to two different ML approaches in the array processing literature. The signals are either regarded as arbitrary unknown sequences, or they are modeled as Gaussian random processes similar to the noise. These two signal models result in the *deterministic* (or conditional) and the *stochastic* (or unconditional) ML methods respectively. In this section, we will briefly review both of these approaches, discuss their relative merits, and present two subspace-based ML approximations. Parametric DOA estimation methods are in general computationally quite complex. However, for ULAs a number of less demanding algorithms are known, as presented in Section 4.4.

4.1 Deterministic Maximum Likelihood

While the background and receiver noise in the assumed data model, can be thought of as emanating from a large number of independent noise sources, the same is usually not the case for the emitter signals. It therefore appears natural to model the noise as a stationary Gaussian white random process whereas the signal waveforms are deterministic (arbitrary) and unknown. Assuming spatially white and circularly symmetric[9] noise, the second-order moments of the noise term take the form

$$\mathrm{E}\{\mathbf{n}(t)\mathbf{n}^H(s)\} = \sigma^2 \mathbf{I}\,\delta_{t,s} \tag{42}$$

$$\mathrm{E}\{\mathbf{n}(t)\mathbf{n}^T(s)\} = 0\,. \tag{43}$$

As a consequence of the statistical assumptions, the observation vector $\mathbf{x}(t)$ is also a circularly symmetric and temporally white Gaussian random process, with mean $\mathbf{A}(\boldsymbol{\theta})\mathbf{s}(t)$ and covariance matrix $\sigma^2\mathbf{I}$. The *likelihood function* is the probability density function (PDF) of all observations given the unknown parameters. The PDF of one measurement

[9] A complex random process is circularly symmetric if its real and imaginary parts are identically distributed and have a skew-symmetric cross-covariance, i.e., $\mathrm{E}[\mathrm{Re}(\mathbf{n}(t))\mathrm{Im}(\mathbf{n}^T(t))] = -\mathrm{E}[\mathrm{Im}(\mathbf{n}(t))\mathrm{Re}(\mathbf{n}^T(t))]$.

vector $\mathbf{x}(t)$ is the complex L-variate Gaussian:

$$\frac{1}{|\pi\sigma^2\mathbf{I}|}\, e^{\|\mathbf{x}(t)-\mathbf{A}\mathbf{s}(t)\|^2/\sigma^2} \;, \tag{44}$$

where $|\cdot|$ denotes the determinant, $\|\cdot\|$ the Euclidean norm, and the argument of $\mathbf{A}(\boldsymbol{\theta})$ has been dropped for notational convenience. Since the measurements are independent, the likelihood function is obtained as

$$L_{DML}(\boldsymbol{\theta}, \mathbf{s}(t), \sigma^2) = \Pi_{t=1}^{N} (\pi\sigma^2)^{-L}\, e^{\|\mathbf{x}(t)-\mathbf{A}\mathbf{s}(t)\|^2/\sigma^2} \;. \tag{45}$$

As indicated above, the unknown parameters in the likelihood function are the signal parameters $\boldsymbol{\theta}$, the signal waveforms $\mathbf{s}(t)$ and the noise variance σ^2. The ML estimates of these unknowns are calculated as the maximizing arguments of $L(\boldsymbol{\theta}, \mathbf{s}(t), \sigma^2)$, the rationale beeing that these values make the observations as probable as possible. For convenience, the ML estimates are alternatively defined as the minimizing arguments of the negative log-likelihood function $-\log L(\boldsymbol{\theta}, \mathbf{s}(t), \sigma^2)$. Normalizing by N and ignoring the parameter-independent $L \log \pi$-term, we get

$$l_{DML}(\boldsymbol{\theta}, \mathbf{s}(t), \sigma^2) = L \log \sigma^2 + \frac{1}{\sigma^2 N} \sum_{t=1}^{N} \|\mathbf{x}(t) - \mathbf{A}\mathbf{s}(t)\|^2 \;, \tag{46}$$

whose minimizing arguments are the deterministic maximum likelihood (DML) estimates.

As shown in [14, 122], explicit minima with respect to σ^2 and $\mathbf{s}(t)$ can be obtained as

$$\hat{\sigma}^2 = \frac{1}{L}\mathrm{Tr}\{\boldsymbol{\Pi}_{\mathbf{A}}^{\perp}\hat{\mathbf{R}}\} \tag{47}$$

$$\hat{\mathbf{s}}(t) = \mathbf{A}^{\dagger}\mathbf{x}(t) \;, \tag{48}$$

where $\hat{\mathbf{R}}$ is the sample covariance matrix, $\mathbf{A}^{\dagger}$ is the Moore-Penrose pseudo-inverse of $\mathbf{A}$ and $\boldsymbol{\Pi}_{\mathbf{A}}^{\perp}$ is the orthogonal projector onto the nullspace of $\mathbf{A}^H$, i.e.

$$\hat{\mathbf{R}} = \frac{1}{N}\sum_{t=1}^{N} \mathbf{x}(t)\mathbf{x}^H(t) \tag{49}$$

$$\mathbf{A}^{\dagger} = (\mathbf{A}^H\mathbf{A})^{-1}\mathbf{A}^H \tag{50}$$

$$\boldsymbol{\Pi}_{\mathbf{A}} = \mathbf{A}\mathbf{A}^{\dagger} \tag{51}$$

$$\boldsymbol{\Pi}_{\mathbf{A}}^{\perp} = \mathbf{I} - \boldsymbol{\Pi}_{\mathbf{A}} \;. \tag{52}$$

Substituting (47)–(48) into (45) shows that the DML signal parameter estimates are obtained by solving the following minimization problem:

$$\hat{\boldsymbol{\theta}}_{DML} = \arg\left\{\min_{\boldsymbol{\theta}} \mathrm{Tr}\{\boldsymbol{\Pi}_{\mathbf{A}}^{\perp}\hat{\mathbf{R}}\}\right\} \;. \tag{53}$$

The interpretation is that the measurements $\mathbf{x}(t)$ are projected onto a model subspace orthogonal to all anticipated signal components, and a power measurement $\frac{1}{N}\sum_{t=1}^{N}\|\mathbf{\Pi}_{\mathbf{A}}^{\perp}\mathbf{x}(t)\| = \mathrm{Tr}\{\mathbf{\Pi}_{\mathbf{A}}^{\perp}\hat{\mathbf{R}}\}$ is evaluated. The energy should clearly be smallest when the projector indeed removes all the true signal components, i.e., when $\boldsymbol{\theta} = \boldsymbol{\theta}_0$. Since only a finite number of noisy samples is available, the energy is not perfectly measured and $\hat{\boldsymbol{\theta}}_{DML}$ will deviate from $\boldsymbol{\theta}_0$. However, if the scenario is stationary, the error will converge to zero as the number of samples is increased to infinity . This remains valid for correlated or even coherent signals, although the accuracy in finite samples is somewhat dependent upon signals correlations.

To calculate the DML estimates, the non-linear M-dimensional optimization problem (46) must be solved numerically. Finding the signal waveform and noise variance estimates (if desired) is then straightforward, by inserting $\hat{\boldsymbol{\theta}}_{DML}$ into (47)–(48). Given a good initial guess, a Gauss-Newton technique (see e.g. [22, 118]) usually converges rapidly to the minimum of (46). Obtaining sufficiently accurate initial estimates, however, is generally a computationally expensive task. If these are poor, the search procedure may converge to a local minimum, and never reach the desired global minimum. A spectral-based method (see Section 3) is a natural choice for an initial estimator, provided all sources can be resolved. Another possibility is to apply the alternating projection technique of [141]. However, convergence to the global minimum can still not be guaranteed. Some more aspects on the global properties of the criteria can be found in [77].

4.2 Stochastic Maximum Likelihood

The other ML technique reported in the literature is termed the stochastic maximum likelihood (SML) method. This method is obtained by modeling the signal waveforms as Gaussian random processes. This model is reasonable, for instance, if the measurements are obtained by filtering wideband signals using a narrow bandpass filter data. It is, however, important to point out that the method is applicable even if the data is not Gaussian. In fact, the asymptotic (for large samples) accuracy of the signal parameter estimates can be shown to depend only on the second-order properties (powers and correlations) of the signal waveforms [100, 76]. With this in mind, the Gaussian signal assumption is merely a way to obtain a tractable ML method. Let the signal waveforms be zero-mean with second-order properties

$$\mathrm{E}\{\mathbf{s}(t)\mathbf{s}^H(s)\} = \mathbf{P}\,\delta_{t,s} \tag{54}$$

$$\mathrm{E}\{\mathbf{s}(t)\mathbf{s}^T(s)\} = 0\,. \tag{55}$$

Then, the observation vector $\mathbf{x}(t)$ is a white, zero-mean and circularly symmetric Gaussian random vector with covariance matrix

$$\mathbf{R} = \mathbf{A}(\boldsymbol{\theta})\mathbf{P}\mathbf{A}^H(\boldsymbol{\theta}) + \sigma^2\mathbf{I}\,. \tag{56}$$

The set of unknown parameters is in this case, different from that in the deterministic signal model. Now, the likelihood function depends on $\boldsymbol{\theta}$, $\mathbf{P}$ and σ^2. The negative log-

likelihood function (ignoring constant terms) is in this case easily shown to be

$$l_{SML}(\boldsymbol{\theta}, \mathbf{P}, \sigma^2) = \log|\mathbf{R}| + \mathrm{Tr}\{\mathbf{R}^{-1}\hat{\mathbf{R}}\} \ . \tag{57}$$

Though this is a highly non-linear function, this criterion allows explicit separation of some of the parameters. For fixed $\boldsymbol{\theta}$, the minimum with respect to σ^2 and $\mathbf{P}$ can be shown to be (although this requires some tedious calculations [15, 51])

$$\hat{\sigma}^2_{SML}(\boldsymbol{\theta}) = \frac{1}{L-M}\mathrm{Tr}\{\boldsymbol{\Pi}^{\perp}_{\mathbf{A}}\hat{\mathbf{R}}\} \tag{58}$$

$$\hat{\mathbf{P}}_{SML}(\boldsymbol{\theta}) = \mathbf{A}^{\dagger}(\hat{\mathbf{R}} - \hat{\sigma}^2_{SML}(\boldsymbol{\theta})\,\mathbf{I})\mathbf{A}^{\dagger H} \ . \tag{59}$$

When (58)–(59) are substituted into (57), the following compact form of the criterion is obtained

$$\hat{\boldsymbol{\theta}}_{SML} = \arg\left\{\min_{\boldsymbol{\theta}} \log\left|\ \mathbf{A}\hat{\mathbf{P}}_{SML}(\boldsymbol{\theta})\mathbf{A}^{H} + \hat{\sigma}^2_{SML}(\boldsymbol{\theta})\,\mathbf{I}\ \right|\right\} \ . \tag{60}$$

In addition this criterion has a nice interpretation, namely that the determinant $\left|\ \mathbf{A}\hat{\mathbf{P}}_{SML}(\boldsymbol{\theta})\mathbf{A}^{H} + \hat{\sigma}^2_{SML}(\boldsymbol{\theta})\,\mathbf{I}\ \right|$, termed the *generalized variance* in the literature, measures the volume of a confidence interval for the data vector. Note that the argument of the determinant is the structured ML estimate of the array covariance matrix! Consequently, we are looking for the model occupying the least volume, to obtain the "cheapest possible" explanation of the data.

The criterion function in (60) is also a higly non-linear function of its argument $\boldsymbol{\theta}$. A Newton-type technique implemention of the numerical search is reported in [77] and an excellent statistical accuracy results when the global minimum is attained. Indeed, the SML signal parameter estimates have been shown to have a better large sample accuracy than the corresponding DML estimates [100, 76], with the difference being significant only for small numbers of sensors, low SNR and highly correlated signals. This is true regardless of the actual distribution of the signal waveforms, in particular they need not be Gaussian. For Gaussian signals, the SML estimates attain the Cramér-Rao lower bound (CRB) on the estimation error variance, derived under the stochastic signal model. This follows from the general theory of ML estimation (see e.g. [112]), since all unknowns in the stochastic model are estimated consistently. The situation is different in the deterministic model for which the number of signal waveform parameters $\mathbf{s}(t)$ grows without bound as the number of samples increases: they cannot be consistently estimated. Hence, the general ML theory does not apply and the DML estimates do not attain the corresponding ("deterministic") CRB.

4.3 Subspace-Based Approximations

As noted in Section 3, subspace-based methods offer significant performance improvements in comparison to conventional beamforming methods. In fact, the MUSIC method has been shown to yield estimates with a large-sample accuracy identical to that of the DML method, provided the emitter signals are uncorrelated [97]. The spectral-based

methods, however, usually suffer from a large bias in finite samples, leading to resolution problems. This problem is accentuated for increasing source correlation. Recently, parametric subspace-based methods that practically have the same statistical performance as the ML methods have been developed [101, 102, 117, 118]. The computational cost for these so-called *Subspace Fitting* methods is, however, less than for the ML dito. As will be seen in Section 4.4.3, a computationally attractive implementation is known for the ubiquitous case of a uniform linear array.

Recall the structure of the eigendecomposition of the array covariance matrix (32),

$$\begin{aligned} \mathbf{R} &= \mathbf{A}\mathbf{P}\mathbf{A}^H + \sigma^2\mathbf{I} && (61) \\ &= \mathbf{U}_s\mathbf{\Lambda}_s\mathbf{U}_s^H + \sigma^2\mathbf{U}_n\mathbf{U}_n^H && (62) \end{aligned}$$

As previously noted, the matrices $\mathbf{A}$ and $\mathbf{U}_s$ span the same range space whenever $\mathbf{P}$ has full rank. In the general case, the number of signal eigenvectors in $\mathbf{U}_s$ equals M', the rank of $\mathbf{P}$. The matrix $\mathbf{U}_s$ will then span an M'-dimensional subspace of $\mathbf{A}$. To see this, express the identity in (61) as $\mathbf{I} = \mathbf{U}_s\mathbf{U}_s^H + \mathbf{U}_n\mathbf{U}_n^H$. Cancelling the $\sigma^2\mathbf{U}_n\mathbf{U}_n^H$-term then yields

$$\mathbf{A}\mathbf{P}\mathbf{A}^H + \sigma^2\mathbf{U}_s\mathbf{U}_s^H = \mathbf{U}_s\mathbf{\Lambda}_s\mathbf{U}_s^H \ . \tag{63}$$

Post-multiplying on the right by $\mathbf{U}_s$ (note that $\mathbf{U}_s^H\mathbf{U}_s = \mathbf{I}$) and re-arranging gives the relation

$$\mathbf{U}_s = \mathbf{A}\mathbf{T} \ , \tag{64}$$

where $\mathbf{T}$ is the full-rank $M \times M'$ matrix

$$\mathbf{T} = \mathbf{P}\mathbf{A}^H\mathbf{U}_s(\mathbf{\Lambda}_s - \sigma^2\mathbf{I})^{-1} \ . \tag{65}$$

The relation (64) forms the basis for the *Signal Subspace Fitting* (SSF) approach. Since $\boldsymbol{\theta}$ and $\mathbf{T}$ are unknown, it appears natural to search for the values that solve (64). The resulting $\boldsymbol{\theta}$ will be the true DOAs (under general identifiability conditions [126]), whereas $\mathbf{T}$ is an uninteresting "nuisance parameter". When only an estimate $\hat{\mathbf{U}}_s$ of $\mathbf{U}_s$ is available, there will be no such solution. Instead, we try to minimize some distance measure betwen $\hat{\mathbf{U}}_s$ and $\mathbf{A}\mathbf{T}$. The Frobenius norm, defined as the square-root of the sum of squared moduli of the elements of a matrix, is a useful measure for this purpose. Alternatively, the squared Frobenius norm can be expressed as the sum of the squared Euclidean norms of the rows or columns. The connection to standard least-squares estimators is therefore clear. The SSF estimate is obtained by solving the following non-linear optimization problem:

$$\{\hat{\boldsymbol{\theta}}, \hat{\mathbf{T}}\} = \arg\min_{\boldsymbol{\theta},\mathbf{T}} \|\hat{\mathbf{U}}_s - \mathbf{A}\mathbf{T}\|_F^2 \ . \tag{66}$$

Similar to the DML criterion (46), this is a separable non-linear least squares problem [44]. The solution for the linear parameter $\mathbf{T}$ (for fixed unknown $\mathbf{A}$) is

$$\hat{\mathbf{T}} = \mathbf{A}^\dagger\hat{\mathbf{U}}_s. \tag{67}$$

Substituting (67) into (66) leads to the separated criterion function

$$\hat{\boldsymbol{\theta}} = \arg\left\{\min_{\boldsymbol{\theta}} \mathrm{Tr}\{\boldsymbol{\Pi}_{\mathbf{A}}^{\perp}\hat{\mathbf{U}}_s\hat{\boldsymbol{\Lambda}}_s\hat{\mathbf{U}}_s^H\}\right\} . \tag{68}$$

Since the eigenvectors are estimated with different quality, depending on how close the corresponding eigenvalues are to the noise variance, it is natural to introduce a weighting of the eigenvectors. We thus arrive at the form

$$\hat{\boldsymbol{\theta}}_{SSF} = \arg\left\{\min_{\boldsymbol{\theta}} \mathrm{Tr}\{\boldsymbol{\Pi}_{\mathbf{A}}^{\perp}\hat{\mathbf{U}}_s\mathbf{W}\hat{\mathbf{U}}_s^H\}\right\} . \tag{69}$$

A natural question is how to pick $\mathbf{W}$ to maximize the accuracy, i.e., to minimize the estimation error variance. It can be shown that the projected eigenvectors $\boldsymbol{\Pi}_{\mathbf{A}}^{\perp}(\boldsymbol{\theta}_0)\hat{\mathbf{u}}_k$, $k = 1, \ldots, M'$ are asymptotically independent. Hence, following from the theory of weighted least squares, [43], $\mathbf{W}$ should be a diagonal matrix containing the inverse of the covariance matrix of $\boldsymbol{\Pi}_{\mathbf{A}}^{\perp}(\boldsymbol{\theta}_0)\hat{\mathbf{u}}_k$, $k = 1, \ldots, M'$. This leads to the choice [102, 117]

$$\mathbf{W}_{opt} = (\boldsymbol{\Lambda}_s - \sigma^2\mathbf{I})^2\boldsymbol{\Lambda}_s^{-1} . \tag{70}$$

Since $\mathbf{W}_{opt}$ depends on unknown quantities, we use instead

$$\hat{\mathbf{W}}_{opt} = (\hat{\boldsymbol{\Lambda}}_s - \hat{\sigma}^2\mathbf{I})^2\hat{\boldsymbol{\Lambda}}_s^{-1} , \tag{71}$$

where $\hat{\sigma}^2$ denotes a consistent estimate of the noise variance, for example the average of the $L - M'$ smallest eigenvalues. The estimator defined by (69) with weights given by (71) is termed the *Weighted Subspace Fitting* (WSF) method. It has been shown to theoretically yield the same large sample accuracy as the SML method, and at a lower computational cost provided a fast method for computing the eigendecomposition is used (see Section 5.5). Practical evidence, see e.g. [77], have given by hand that the WSF and SML methods also exhibit similar small sample (i.e. threshold) behaviour.

An alternative subspace fitting formulation is obtained by instead starting from the "MUSIC relation"

$$\mathbf{A}^H(\boldsymbol{\theta})\mathbf{U}_n = 0 \text{ iff } \boldsymbol{\theta} = \boldsymbol{\theta}_0 , \tag{72}$$

which holds for $\mathbf{P}$ having full rank. Given an estimate of $\mathbf{U}_n$, it is natural to look for the signal parameters that minimize the following *Noise Subspace Fitting* (NSF) criterion,

$$\hat{\boldsymbol{\theta}} = \arg\left\{\min_{\boldsymbol{\theta}} \mathrm{Tr}\{\mathbf{A}^H\hat{\mathbf{U}}_n\hat{\mathbf{U}}_n^H\mathbf{A}\mathbf{V}\}\right\} , \tag{73}$$

where $\mathbf{V}$ is some positive (semi-)definite weighting matrix. Interestingly enough, the estimates calculated by (73) and (69) asymptotically coincide , if the weighting matrices are (asymptotically) related by [77]

$$\mathbf{V} = \mathbf{A}^{\dagger}(\boldsymbol{\theta}_0)\hat{\mathbf{U}}_s\mathbf{W}\hat{\mathbf{U}}_s^H\mathbf{A}^{\dagger *}(\boldsymbol{\theta}_0) . \tag{74}$$

Note also that the NSF method reduces to the MUSIC algorithm for $\mathbf{V} = \mathbf{I}$, provided $|\mathbf{a}(\theta)|$ is independent of θ. Thus, in a sense the general estimator in (73) unifies the parametric methods and also encompasses the spectral-based subspace methods.

The NSF method has the advantage that the criterion function in (73) is a quadratic function of the steering matrix $\mathbf{A}$. This is useful if any of the parameters of $\mathbf{A}$ enter linearly. An analytical solution with respect to these parameters is then readily available (see e.g. [119]). However, this happens only in very special situations, rendering this forementioned advantage of limited importance. The NSF formulation is also fraught with some drawbacks, namely that it cannot produce reliable estimates for coherent signals, and that the optimal weighting $\mathbf{V}_{opt}$ depends on $\boldsymbol{\theta}_0$, so that a two-step procedure has to be adopted.

4.4 Uniform Linear Arrays

The steering matrix for a uniform linear array has a very special, and as it turns out, useful structure, which, as described next, will result in enhanced performance. From (28), the ULA steering matrix takes the form

$$\mathbf{A}(\boldsymbol{\theta}) = \begin{bmatrix} 1 & 1 & \cdots & 1 \\ e^{j\phi_1} & e^{j\phi_2} & \cdots & e^{j\phi_M} \\ \vdots & \vdots & & \vdots \\ e^{j(L-1)\phi_1} & e^{j(L-1)\phi_2} & \cdots & e^{j(L-1)\phi_M} \end{bmatrix} . \tag{75}$$

This structure is referred to as a *Vandermonde matrix* [44].

4.4.1 Root-MUSIC

The Root-MUSIC method [11], as the name implies, is a polynomial-rooting version of the orginal MUSIC technique. The idea dates back to Pisarenko's method [81]. The basic observation is that the polynomial

$$p_k(z) = \mathbf{u}_k^H \mathbf{a}(z) \; k = M+1, M+2, \ldots, L \; , \tag{76}$$

where

$$\mathbf{a}(z) = [1, z, \ldots, z^{L-1}]^T \; , \tag{77}$$

has M of its zeros at $e^{j\phi_l}$, $l = 1, 2, \ldots, M$ provided that $\mathbf{P}$ has full rank. To exploit the information from all noise eigenvectors simultaneously, we want to find the zeros of the MUSIC function

$$\|\hat{\mathbf{U}}_n^H \mathbf{a}(z)\|^2 = \mathbf{a}^H(z) \hat{\mathbf{U}}_n \hat{\mathbf{U}}_n^H \mathbf{a}(z) \; . \tag{78}$$

However, the latter function is not a polynomial in z, which complicates the search for zeros. Since we are interested in values of z on the unit circle, we can use $\mathbf{a}^T(z^{-1})$ for $\mathbf{a}^H(z)$, which gives the Root-MUSIC polynomial

$$P(z) = z^L \, \mathbf{a}^T(z^{-1}) \hat{\mathbf{U}}_n \hat{\mathbf{U}}_n^H \mathbf{a}(z) \mathbf{a}^H(z) \; . \tag{79}$$

Note that $P(z)$ will have M roots inside the unit circle (UC), that have M mirrored images outside the UC. Of the ones inside, the phases of the M closest to the UC, say $\hat{z}_1, \hat{z}_2, \ldots, \hat{z}_M$, yield the DOA estimates, as

$$\hat{\theta}_k = -\arcsin\left(\frac{c}{\omega} d \arg(\hat{z}_k)\right) . \tag{80}$$

It has been shown [97, 98] that MUSIC and Root-MUSIC have identical asymptotic properties, although in small samples Root-MUSIC has empirically been found to perform significantly better. As previously alluded to, this can be attributed to a larger bias for spectral-based methods, as compared to the parametric techniques [62, 85].

4.4.2 ESPRIT

The ESPRIT algorithm [80, 87] uses the structure of the ULA steering vectors in a slightly different way. The observation here is that $\mathbf{A}$ has a so-called *shift structure*. Define the sub-matrices $\mathbf{A}_1$ and $\mathbf{A}_2$ by deleting the first and last rows from $\mathbf{A}$ respectively, i.e.

$$\mathbf{A} = \begin{bmatrix} \mathbf{A}_1 \\ \text{last row} \end{bmatrix} = \begin{bmatrix} \text{first row} \\ \mathbf{A}_2 \end{bmatrix} . \tag{81}$$

By the structure (75), $\mathbf{A}_1$ and $\mathbf{A}_2$ are related by the formula

$$\mathbf{A}_2 = \mathbf{A}_1 \mathbf{\Phi} , \tag{82}$$

where $\mathbf{\Phi}$ is a diagonal matrix having the "roots" $e^{j\phi_k}$, $k = 1, 2, \ldots, M$ on the diagonal. Thus, the DOA estimation problem can be reduced to that of finding $\mathbf{\Phi}$. Like the other subspace-based algorithms, ESPRIT relies on properties of the eigendecomposition of the array covariance matrix. Recall the relation (64). Deleting the first and last rows of (64) respectively, we get

$$\mathbf{U}_1 = \mathbf{A}_1 \mathbf{T} \quad , \quad \mathbf{U}_2 = \mathbf{A}_2 \mathbf{T} , \tag{83}$$

where $\mathbf{U}_s$ has been partitioned conformably with $\mathbf{A}$ into the sub-matrices $\mathbf{U}_1$ and $\mathbf{U}_2$. Combining (82) and (83) yields

$$\mathbf{U}_2 = \mathbf{A}_1 \mathbf{\Phi} \mathbf{T} = \mathbf{U}_1 \mathbf{T}^{-1} \mathbf{\Phi} \mathbf{T} . \tag{84}$$

Finally, defining $\mathbf{\Psi} = \mathbf{T}^{-1} \mathbf{\Phi} \mathbf{T}$ we obtain

$$\mathbf{U}_2 = \mathbf{U}_1 \mathbf{\Psi} . \tag{85}$$

Note that $\mathbf{\Psi}$ and $\mathbf{\Phi}$ are related by a similarity transformation, and hence have the same eigenvalues. The latter are of course given by $e^{j\phi_k}$, $k = 1, 2, \ldots, M$, and are related to the DOAs by (80). The ESPRIT algorithm is now stated:

1. Compute the eigendecomposition of the array covariance matrix
2. Form $\hat{\mathbf{U}}_1$ and $\hat{\mathbf{U}}_2$ from the M principal eigenvectors

3. Solve the approximate relation (85) in either a Least-Squares sense (LS-ESPRIT) or a Total-Least-Squares [43, 44] sense (TLS-ESPRIT)

4. The DOA estimates are obtained by applying the inversion formula (80) to the eigenvalues of $\hat{\mathbf{\Psi}}$

It has been shown that LS-ESPRIT and TLS-ESPRIT yield identical asymptotic estimation accuracy [84], although in small samples TLS-ESPRIT usually has an edge.

4.4.3 IQML and Root-WSF

Another interesting exploitation of the ULA structure was presented in [17], although the idea can be traced back to the Steiglitz and McBride algorithm for system identification [96]. The IQML algorithm is an iterative procedure for minimizing the DML criterion

$$V(\boldsymbol{\theta}) = \mathrm{Tr}\{\mathbf{\Pi}_{\mathbf{A}}^{\perp}\hat{\mathbf{R}}\} \ . \tag{86}$$

The idea is to re-parametrize the projection matrix $\mathbf{\Pi}_{\mathbf{A}}^{\perp}$ using a basis for the nullspace of $\mathbf{A}^H$. Towards this end, define the polynomial $b(z)$ to have its M roots at $e^{j\phi_k}$, $k = 1, 2, \ldots, M$, i.e.,

$$b(z) = z^M + b_1 z^{M-1} + \cdots + b_M = \Pi_{k=1}^{M}(z - e^{j\phi_k}) \tag{87}$$

Then, by construction the following relation holds true

$$\begin{bmatrix} b_M & b_{M-1} & \cdots & 1 & \cdots & 0 \\ & \ddots & \ddots & & \ddots & \\ 0 & & b_M & b_{M-1} & \cdots & 1 \end{bmatrix} \begin{bmatrix} 1 & \cdots & 1 \\ e^{j\phi_1} & \cdots & e^{j\phi_M} \\ \vdots & \vdots & \vdots \\ e^{j(L-1)\phi_1} & \cdots & e^{j(L-1)\phi_M} \end{bmatrix} = 0 \tag{88}$$

$$\Leftrightarrow \quad \mathbf{B}^H\mathbf{A} = 0 \ .$$

Since $\mathbf{B}$ has full rank $L - M$, its columns do in fact form a basis for the nullspace of $\mathbf{A}^H$. Apparently the orthogonal projections onto these subspaces must coincide, implying

$$\mathbf{\Pi}_{\mathbf{A}}^{\perp} = \mathbf{B}(\mathbf{B}^H\mathbf{B})^{-1}\mathbf{B}^H \ . \tag{89}$$

Now the DML criterion function can be parametrized by the polynomial coefficients b_k in lieu of the DOAs θ_k. The DML estimate (53) can be calculated by solving

$$\hat{\mathbf{b}} = \arg\min_{\mathbf{b}} \mathrm{Tr}\{\mathbf{B}(\mathbf{B}^H\mathbf{B})^{-1}\mathbf{B}^H\hat{\mathbf{R}}\} \tag{90}$$

and then applying (80) to the roots of the estimated polynomial. Unfortunately, (90) is still a difficult non-linear optimization problem. However, [17] suggested an iterative solution as follows

1. Set $\mathbf{U} = \mathbf{I}$

2. Solve the quadratic problem

$$\hat{\mathbf{b}} = \arg\min_{\mathbf{b}} \mathrm{Tr}\{\mathbf{B}\mathbf{U}\mathbf{B}^H\hat{\mathbf{R}}\} \tag{91}$$

3. Form $\hat{\mathbf{B}}$ and put $\mathbf{U} = (\hat{\mathbf{B}}^H\hat{\mathbf{B}})^{-1}$

4. Check for convergence. If not, goto Step 2

5. Apply (80) to the roots of $\hat{b}(z)$.

Since the roots of $b(z)$ should be on the UC, [18] suggested using the constraint

$$b_k = b_{M-k}^H, \ k = 1, 2, \ldots, M \tag{92}$$

when solving (91). Now, (92) does not guarantee roots on the UC, but it can be shown that the accuracy loss due to this fact is negligible. While the above described IQML (Iterative Quadratic Maximum Likelihood) algorithm cannot be guaranteed to converge, it has indeed been found to perform well in simulations.

An improvement over IQML was introduced in [101]. The idea is simply to apply the IQML iterations to the WSF criterion (69). Since the criteria have the same form, the modification is straightforward. However, there is a very important advantage of using the rank-truncated form $\hat{\mathbf{U}}_s\mathbf{W}\hat{\mathbf{U}}_s^H$ rather than $\hat{\mathbf{R}}$ in (91). That is, after the second pass of the iterative scheme, the estimates already have the asymptotic accuracy of the true optimum! Hence, the resulting IQ-WSF algorithm is no longer an iterative procedure:

1. Solve the quadratic problem

$$\hat{\mathbf{b}} = \arg\min_{\mathbf{b}} \mathrm{Tr}\{\mathbf{B}\mathbf{B}^H\hat{\mathbf{U}}_s\mathbf{W}\hat{\mathbf{U}}_s^H\} \tag{93}$$

2. Solve the quadratic problem

$$\hat{\mathbf{b}} = \arg\min_{\mathbf{b}} \mathrm{Tr}\{\mathbf{B}(\hat{\mathbf{B}}^H\hat{\mathbf{B}})^{-1}\mathbf{B}^H\hat{\mathbf{U}}_s\mathbf{W}\hat{\mathbf{U}}_s^H\} \tag{94}$$

3. Apply (80) to the roots of $\hat{b}(z)$.

Note that this algorithm is essentially in closed form (if one accepts solving for the eigen-decomposition and polynomial rooting as closed form), and that the resulting estimates have the best possible asymptotic accuracy. Thus, the IQ-WSF algorithm is a strong candidate for the "best" method for ULAs.

5 Additional Topics

The emphasis in this paper is on computational methods for sensor array processing. Because of space limitations, we have omitted several interesting topics from the main discussion and instead give a very brief overview of these additional topics in this section. We structure this section in the form of a commented enumeration of references to selected specialized papers.

5.1 Number of Signals Estimation

In applications of model-based methods, an important problem is the determination of M, the number of signals. In the case of non-coherent signals, the number of signals is equal to the number of "large" eigenvalues of the array covariance matrix. This fact is used to obtain relatively simple non-parametric algorithms for determining M. The most frequently used approach emanates from the factor analysis literature [4]. The idea is to determine the multiplicity of the smallest eigenvalue, which theoretically equals $L - M$. A statistical hypothesis test is proposed in [91], whereas [124, 140] are based on information theoretic criteria, such as Akaike's AIC (an information theoretic criterion) and Rissanen's MDL (minimum description length). Unfortunately, the above mentioned approach is very sensitive to the assumption of a spatially white noise field [136]. An alternative idea based on using the eigenvectors rather than the eigenvalues is pursued in the referenced paper. Another non-parametric method is presented in [29].

In the presence of coherent signals, the above mentioned methods will fail as stated, since the dimension of the signal subspace then is smaller than M. However, for ULAs one can test the eigenvalues of the spatially smoothed array covariance matrix to determine M [93], with further improved performance in [61].

A more systematic approach to estimating the number of signals is possible if the maximum likelihood estimator is employed. A classical generalized likelihood ratio test (GLRT) is described in [77], whereas [123] presents an information theoretic approach. Another model-based detection technique is presented in [118, 77], based on the weighted subspace fitting method. The model-based methods for determining the number of signals require calculating signal parameter estimates for an increasing hyphotesized numbers of signals, until some pre-specified criterion is met. Hence, the approach is inherently more computationally complex than the non-parametric tests. Its performance in difficult signal scenarios is, however, improved and the model-based technique is less sensitive to small perturbations of the assumed noise covariance matrix.

5.2 Reduced Dimension Beamspace Processing

Except for the beamforming-based methods, the estimation techniques discussed herein require that the outputs of all elements of the sensor array be available in digital form. In many applications, the required number of high-precision receiver front-ends and A/D converters may be prohibitive. Arrays of 10^4 elements are not uncommon, for example in

radar applications. Techniques for reducing the dimensionality of the observation vector with minimal effect on performance, is therefore of great interest. As already discussed in Section 3.2.3, a useful idea is to employ a linear transformation

$$\mathbf{z}(t) = \mathbf{T}^*\mathbf{x}(t)\,,$$

where $\mathbf{T}$ is $L \times R$, with (usually) $R \ll L$. The transformation is typically implemented in analog hardware, thus significantly reducing the number of required A/D converters. The reduced-dimension observation vector $\mathbf{z}(t)$ is usually referred to as the *beamspace* data, and $\mathbf{T}$ is a *beamspace transformation.*

Naturally, processing the beamspace data significantly reduces the computational load of the digital processor. However, reducing the dimension of the data also implies a loss of information. The beamspace transformation can be thought of as a multichannel beamformer. By designing the beamformers (the columns of $\mathbf{T}$) so that they focus on a relatively narrow DOA sector, the essential information in $\mathbf{x}(t)$ regarding sources in that sector can be retained in $\mathbf{z}(t)$. See e.g., [38, 116, 138, 142] and the references therein. With further *a priori* information on the locations of sources, the beamspace transformation can in fact be performed without losing any information at all [5]. As previously alluded to, beamspace processing can even *improve* the resolution (the bias) of spectral-based methods.

Note that the beamspace transformation effectively changes the array propagation vectors from $\mathbf{a}(\theta)$ into $\mathbf{T}^*\mathbf{a}(\theta)$. It is possible to utilize this freedom to give the beamspace array manifold a simpler form, such as that of a ULA, [40]. Hence, the computationally efficient ULA techniques (see Section 3 are applicable in beamspace. In [71], a transformation that maps a uniform circlar array into a ULA is proposed and analyzed, enabling computationally efficient estimation of both azimuth and elevation.

5.3 Estimation Under Model Uncertainty

As implied by the terminology, model-based signal processing relies on the availability of a precise mathematical description of the measured data. When the model fails to reflect the physical phenomena with a sufficient accuracy, the performance of the methods will of course degrade. In particular, deviations from the assumed model will introduce bias in the estimates, which for spectral-based methods is manifested by a loss of resolving power and a presence of spurious peaks. In principle, the various sources of modeling errors can be classified into noise covariance and array response perturbations.

In many applications of interest, such as communication, sonar and radar, the background noise is dominated by man-made noise. While the noise generated in the receiving equipment is likely to fulfill the spatially white assumption, the man-made noise tends to be quite directional. The performance degradation under noise modeling errors is studied in, e.g. [68, 121]. One could in principle envision extending the model-based estimation techniques to also include estimation of the noise covariance matrix. Such an approach has the potential of improving the robustness to errors in the assumed noise model [131, 123]. However, for low SNR's, this solution is less than adequate. The simultaneous estimation

of a completely unknown noise covariance matrix and of the signal parameters poses a problem unless some additional information which enables us to separate signal from noise, is available. It is, for example, always possible to infer that the received data is nothing but noise, and that the (unknown) noise covariance matrix is precisely the observed array sample covariance matrix. Estimation of a parametric (structured) noise models is considered in, e.g. [16, 57]. So-called instrumental variable techniques are proposed, e.g. in [104] (based on assumptions on the temporal correlation of signals and noise) and [132] (utilizing assumptions on the spatial correlation of the signals and noise). Methods based on other assumptions appeared in [79, 114].

At high SNR, the modeling errors are usually dominated by errors in the assumed signal model. The signals have a non-zero bandwidth, the sensor positions may be uncertain, the receiving equipment may not be perfectly calibrated, etc. The effects of such errors is studied e.g. in [39, 67, 108, 109]. In some cases it is possible to physically quantify the error sources. A "self-calibrating" approach may then be applicable [86, 127, 119], albeit at a quite a computational cost. In [108, 109, 120], robust techniques for unstructured sensor modeling errors are considered.

5.4 Wideband Data Processing

The methods presented herein are essentially limited to processing narrowband[10] data. In many applications (e.g. radar and communication), this is indeed a realistic assumption. However, in other cases (e.g. sonar), the received signal may be broadband. A natural extension of methods for narrowband data is to employ narrowband filtering, for example using the Fast Fourier Transform (FFT). An optimal exploitation of the data entails combining information from different frequency bins [59], see also [125]. A simpler suboptimal approach is to process the different FFT channels separately using a standard narrowband method, whereafter the DOA estimates at different bins must be somehow combined.

Another approach is to explicitly model the array output as a multidimensional time series, using an auto-regressive moving average (ARMA) model. The poles of the system are estimated, e.g. using the overdetermined Yule-Walker equations. A narrowband technique can subsequently be employed using the estimated spectral density matrix, evaluated at the system poles. In [106], the MUSIC algorithm is applied, whereas [75] proposes to use the ESPRIT algorithm.

A wideband DOA estimation approach inspired by beamspace processing is the so-called coherently averaged signal subspace method. The idea is to first estimate the signal subspace at a number of FFT channels. Then, the information from different frequency bins is merged by employing linear transformations. The objective is to make the transformed steering matrices $\mathbf{A}$ at different frequencies as identical as possible, for example by focusing at the center frequency of the signals. See, e.g. [50, 94] for further details.

[10] Signals whose bandwidths are much smaller than the inverse of the time it takes a wavefront to propagate across the array, are referred to as narrowband.

5.5 Fast Subspace Calculation and Tracking

When implementing subspace-based methods in applications with real-time operation, the bottleneck is usually the calculation of the signal subspace. A scheme for fast computation of the signal subspace is proposed in [54], and methods for subspace tracking are considered in [28]. The idea is to exploit the "low-rank plus $\sigma^2\mathbf{I}$" structure of the ideal array covariance matrix. An alternative gradient-based technique for subspace tracking is proposed in [139]. Therein, it is observed that the solution of the constrained optimization problem, $\mathbf{W}$,

$$\begin{aligned} &\max_{\mathbf{W}} \mathrm{Tr}\{\mathbf{W}^*\hat{\mathbf{R}}\mathbf{W}\} \\ &\text{subject to } \mathbf{W}^*\mathbf{W} = \mathbf{I} \end{aligned}$$

spans the signal subspace.

For some methods, estimates of the individual principal eigenvectors are required, in addition to the subspace they span. A number of different methods for eigenvalue/vector[11] tracking is given in [26]. A more recent approach based on exploiting the structure of the ideal covariance is proposed and analyzed in [134]. The so-called fast subspace decomposition (FSD) technique is based on a Lanczos method for calculating the eigendecoposition. It is observed that the Lanczos iterations can be prematurely terminated without any significant performance loss.

5.6 Signal Structure Methods

Most "standard" approaches to array signal processing make no use of any available information of the signal structure. However, many man-made signals have a rich structure that can be used to improve the estimator performance. In digital communication applications, the transmitted signals are often *cyclostationary*, i.e. their autocorrelation functions are periodic. This extra information is exploited in e.g. [1, 133, 90], and algorithms for DOA estimation of cyclostationary signals are derived and analyzed. In this approach, the wideband signals are easily incorporated into the framework, and there can be more signals than sensors, provided not all of them share the same cyclic frequency.

A different approach utilizing signal structure is based on high-order statistics. As is well-known, all information about a Gaussian signal is conveyed in the first and second order moments. However, for non-Gaussian signals, there is potentially more to be gained by using higher moments. This is particularly so if the noise can be regarded as Gaussian. Then, the high-order cumulants will be noise-free, because they vanish for Gaussian signals. Methods based on the fourth-order cumulant are proposed in [82, 24], whereas [92] proposes to use high-order cyclic spectra (for cyclostationary signals).

A common criticism to both methods based on cyclostationarity and those based on high-order statistics is that they require a considerable amount of data to yield reliable

[11] The referenced paper considers tracking of the principal left singular values of the data matrix. Mathematically, but perhaps not numerically, these are identical to the eigenvectors of the sample covariance matrix.

results. This is because the estimated cyclic and high-order moments typically converge more slowly towards their theoretical values as the number of data is increased.

5.7 Time Series Analysis

The DOA estimation problem employing a ULA has strong similarities with time series analysis. Indeed, an important pre-cursor of the MUSIC algorithm is Pisarenko's method [81] for estimation of the frequencies of damped/undamped sinuoids in noise, when given measurements of their covariance function. Likewise, Kung's algorithm for state-space realization of a measured impulse response [65] is an early version of the ESPRIT algorithm. An important difference between the time series case and the (standard) DOA estimation problem is that the time series data is usually estimated using a sliding window. A "sensor array-like data vector" $\mathbf{x}(t)$ is formed from the scalar time series $y(t)$ by using

$$\mathbf{x}(t) = [y(t), y(t+1), \ldots, y(t+L-1)]^T \ .$$

The windowing transformation induces a temporal correlation in the L-dimensional time series $\mathbf{x}(t)$, even if the scalar process $y(t)$ is temporally white. This fact complicates the analysis, as in the case of spatial smoothing in DOA estimation, see e.g. [25, 103, 61].

6 Applications

The research progress of parameter estimation and detection in array processing has resulted in a great diversity of applications, and continues to provide fertile ground for new ones. In this section we discuss three important application areas, and in addition demonstrate the performance of the algorithms on a real data example.

6.1 Personal Communications

Receiving arrays and related estimation/detection techniques have long been used in High Frequency communications. These applications have recently reemerged and received a significant attention by researchers, as a potentially useful "panacea" for numerous problems in personal communications (see e.g. [130, 107, 3, 105]). They are expected to play a key role in accomodating a multiuser communication environment, subject to severe multipath.

One of the most important problems in a multiuser asynchronous environment is the inter-user interference, which can degrade the performance quite severely. This is the case also in a practical Code-Division Multiple Access (CDMA) system, because the varying delays of different users induce non-orthogonal codes. The base stations in mobile communication systems have long been using *spatial diversity* for combatting fading due to the severe multipath. However, using an antenna array of several elements introduces extra degrees of freedom, which can be used to obtain higher selectivity. An adaptive receiving array can be steered in the direction of one user at a time, while simultaneously nulling interference from other users, much in the the same way as the beamforming techniques described in Section 3.

Figure 5 illustrates a personal communication scenario involving severe multipath. The multipath introduces difficulties for conventional adaptive array processing. Undesired cancellation may occur [128], and spatial smoothing may be required to achieve a proper selectivity. In [3], it is proposed to identify all signal paths emanating from each user, whereafter an optimal combination is made. A configuration equivalent to the beamspace array processing with a simple energy differencing scheme serves in localizing incoming users waveforms [89]. This beamspace strategy underlies an adaptive optimization technique proposed in [105], which addresses the problem of mitigating the effects of dispersive time varying channels.

Communication signals have a rich structure that can be exploited for signal separation using antenna arrays. Indeed, the DOAs need not be estimated. Instead, signal structure methods such as the constant-modulus beamformer [45] have been proposed for directly estimating the steering vectors of the signals, thereby allowing for *blind* (i.e., not requiring a training sequence) signal separation. Techniques based on combining beamforming and demodulation of digitally modulated signals have also recently been proposed (see [70, 110, 95, 111]). It is important to note that the various optimal and/or suboptimal proposed methods are of current research interest, and that in practice, many challenging and interesting problems remain to be addressed.

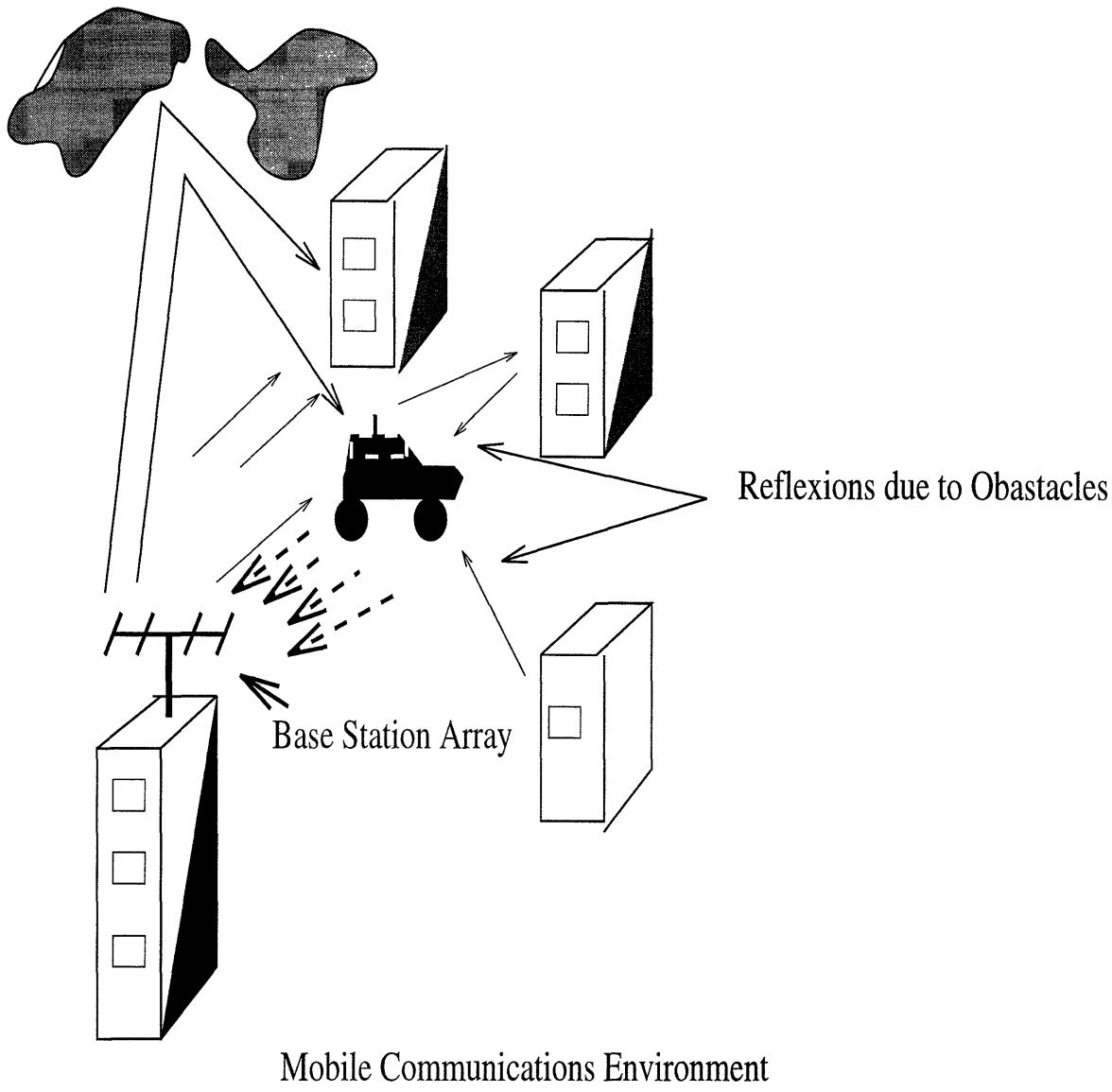

Figure 5: Mobile Radio Scenario with an Adaptive Array

6.2 Radar and Sonar

Modern techniques in array processing have also found an extensive use for in radar and sonar [69, 78, 47, 32, 48]. The antenna array is, for example, used for source localization, interference cancellation and ground clutter suppression.

In radar applications, the mode of operation is referred to as active. This is on account of the role of the antenna array based system which radiates pulses of electromagnetic energy and listens for the return. The parameter space of interest may vary according to

the geometry and sophistication of the antenna array. The radar returns enable estimation of parameters such as velocity, range, direction of arrival of targets of interest [112]. More recently, researchers have focused on an extension of the spatial sampling concept of an array to synthesize a highly resolving array with a moving airborn sensor which periodically transmits/receives electromagnetic energy. Such a *synthetic aperture radar* (SAR) system is pictorially shown in Figure 6.

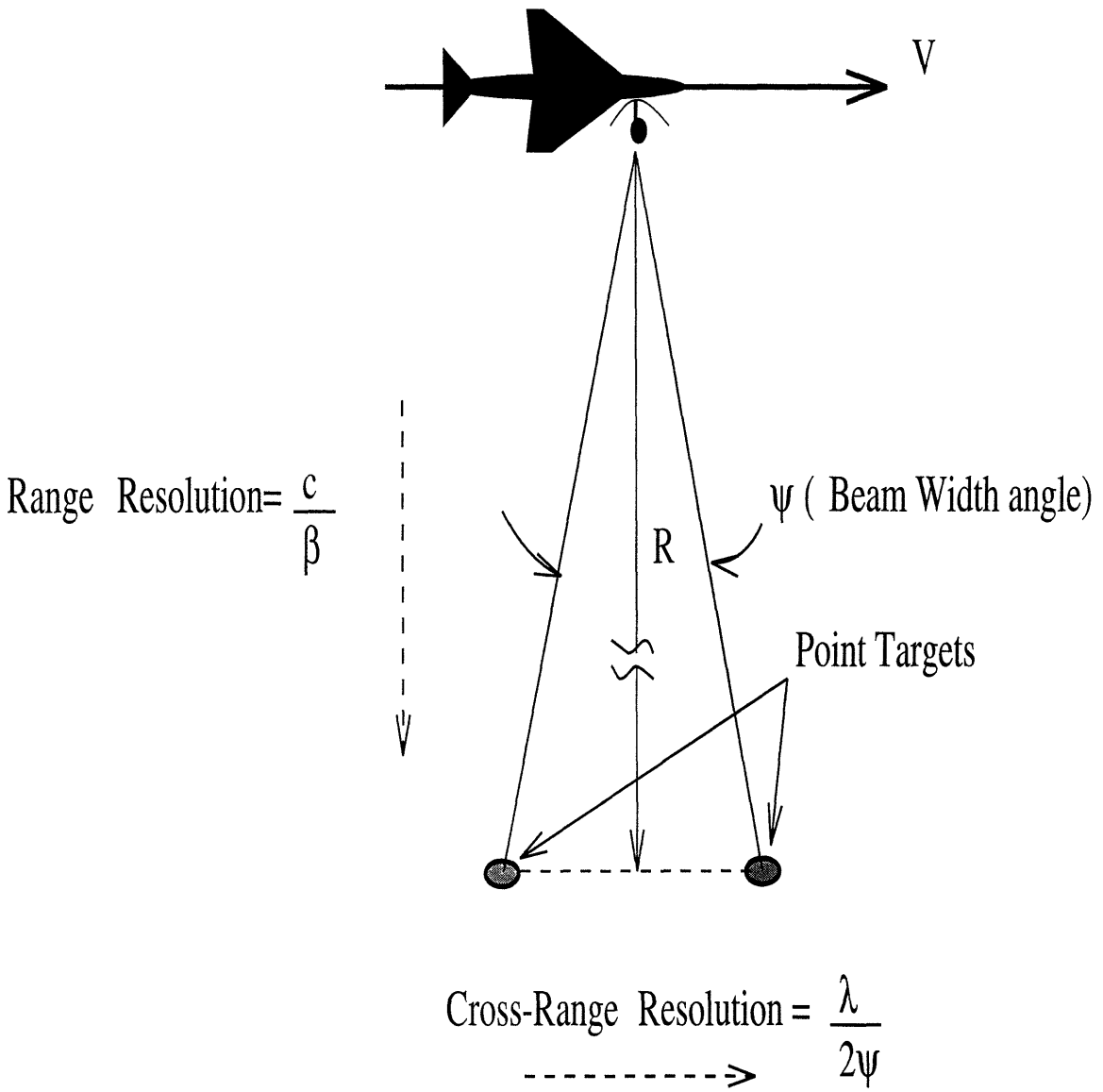

Figure 6: Synthetic Aperture Radar System

The fraction of the scattered energy which is reflected towards the synthesized array, when appropriately processed, i.e. integrated over the range and cross-range (region along

the flight plan), and adequately deconvolved, result in the reflectivity of the background, thus permitting its imaging. Numerous important areas of applications in remote sensing, include *environmental* studies (forrestation etc.), *meteorological* predictions, *oceanography* and many others.

Sonar applications, on the other hand, use acoustic energy and can operate in an active as well as passive mode. In a passive mode, the receiving array is generally in a listening mode to detect and process any acoustic energy emanating from sources. It thus has the capability to locate distant sources. Deformable array models are often used in sonar, as the receiving antenna is typically towed under water [69]. Techniques with piecewise linear subarrays are used in the construction of the overall solution.

In an active mode, a sonar system emits acoustic (electromagnetic arrays are also used underwater) energy and monitors and retrieves whatever echo. This again can be used for parameter estimation, such as bearings and velocity etc., using the delay of the echo. Despite its limitations due to the speed of sound, sonar together with related estimation techniques, remains a reliable tool for range, bearing estimation and other imaging tasks in underwater applications. However, the difficult propagation conditions under water may call for more advanced signal modeling, such as in *matched field processing* (see e.g. [10]).

6.3 Industrial applications

Sensor array signal processing techniques have drawn much interest from industrial applications, such as manufacturing and medical applications. In medical imaging and hyperthermia treatment [35, 36], circular arrays are commonly used as a means to focus energy in both an injection mode as well as reception mode. It has also been used in treatment of tumors [34]. In electrocardiograms, planar arrays are used to track the evolution of wavefronts which in turn provide information about the condition of an individual's heart. Array processing methods have also been adopted to localize brain activity using biomagnetic sensor arrays (SQUID sensors) [74]. It is expected that the medical applications will proliferate as more resolution is sought, e.g. signals emanating from a womb may be of more interest than those of a mother.

Other applications in industry are almost exclusively in automatic monitoring and fault detection/localization. In engines, sensors are placed in a judicious and convenient way to detect and potentially localize faults such as knocks or broken gears [46]. One emerging and important application of array signal processing is in using notions from optics to carry out tasks in product quality assurance in a manufacturing environement [2], and in object shape characterization in tomography [72, 73]. An semiconductor manufactoring example is provided in the following.

As noted earlier, it is often desired to minimize a human input in a manufacturing environment, for a number of reasons (e.g. cost, reliability, etc.). Sensor array processing applications in such an environment have recently been reported. An array of photosensors is used to monitor reflections from a surface, whose image is given in Figure 7. This image could conceptually represent a number of products, but in this case it is that

of a semiconductor wafer which bears a scratch which, for obvious reasons needs to be detected and its position estimated. In Figures 8 and 9, the ESPRIT method is used to estimate the parameters of the diagonal line, namely the coordinates (pixel offset from the left upper corner) as well as the angle of inclination with respect to the vertical. In these Figures, the parametric solution is compared to a more conventional non-parametric method that is more well-known in the area of tomography – the Hough transform. The ESPRIT method performs at least as good as the Hough transform, and on account of its simple implementation, ESPRIT is a promising technique for such applications. Note that the Hough transform requires a great deal of data which in turn is memory intensive, while the computational as well as the storage requirements with ESPRIT is much more advantageous.

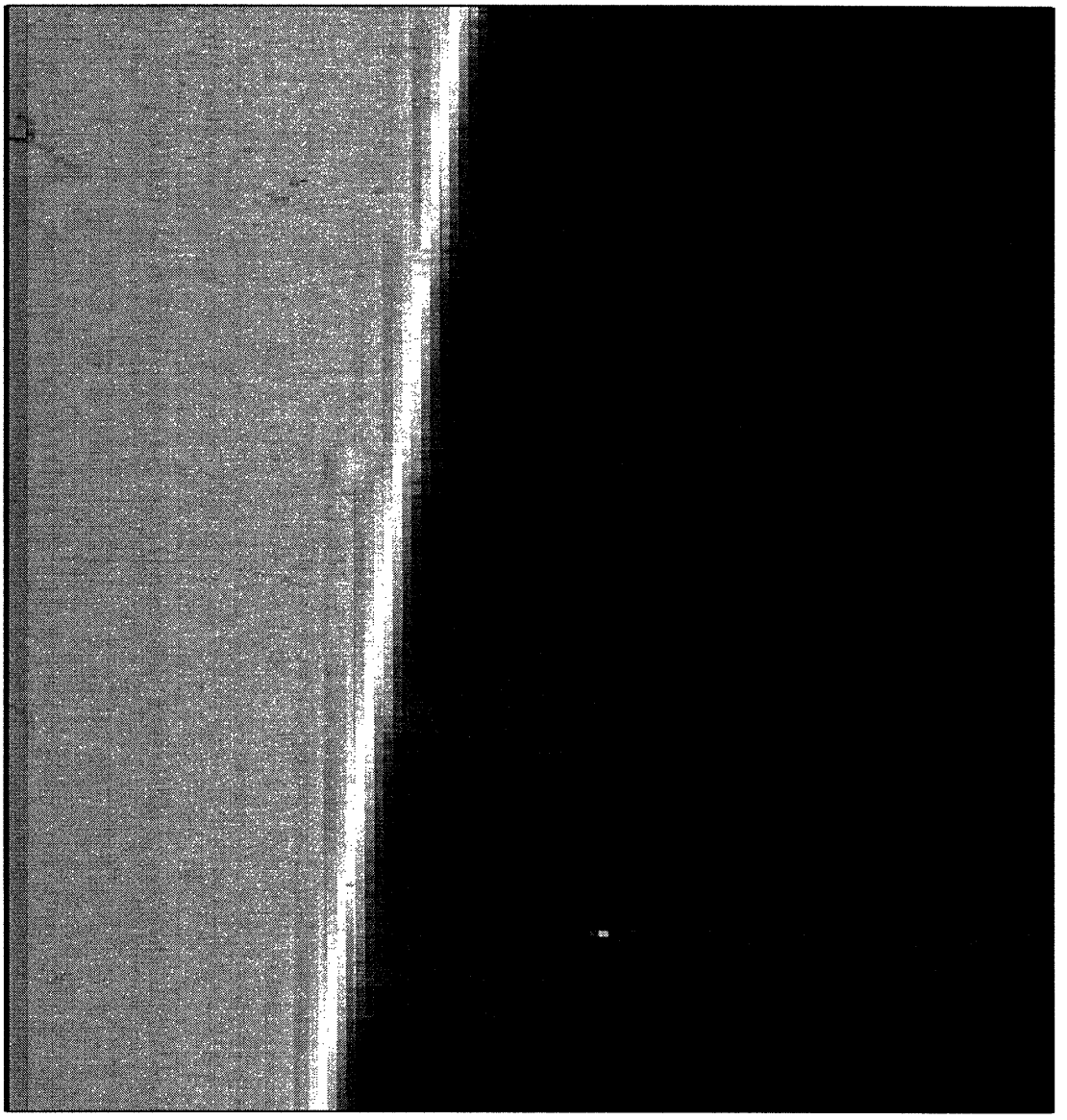

Figure 7: *Semiconductor chip with an inscribed line*

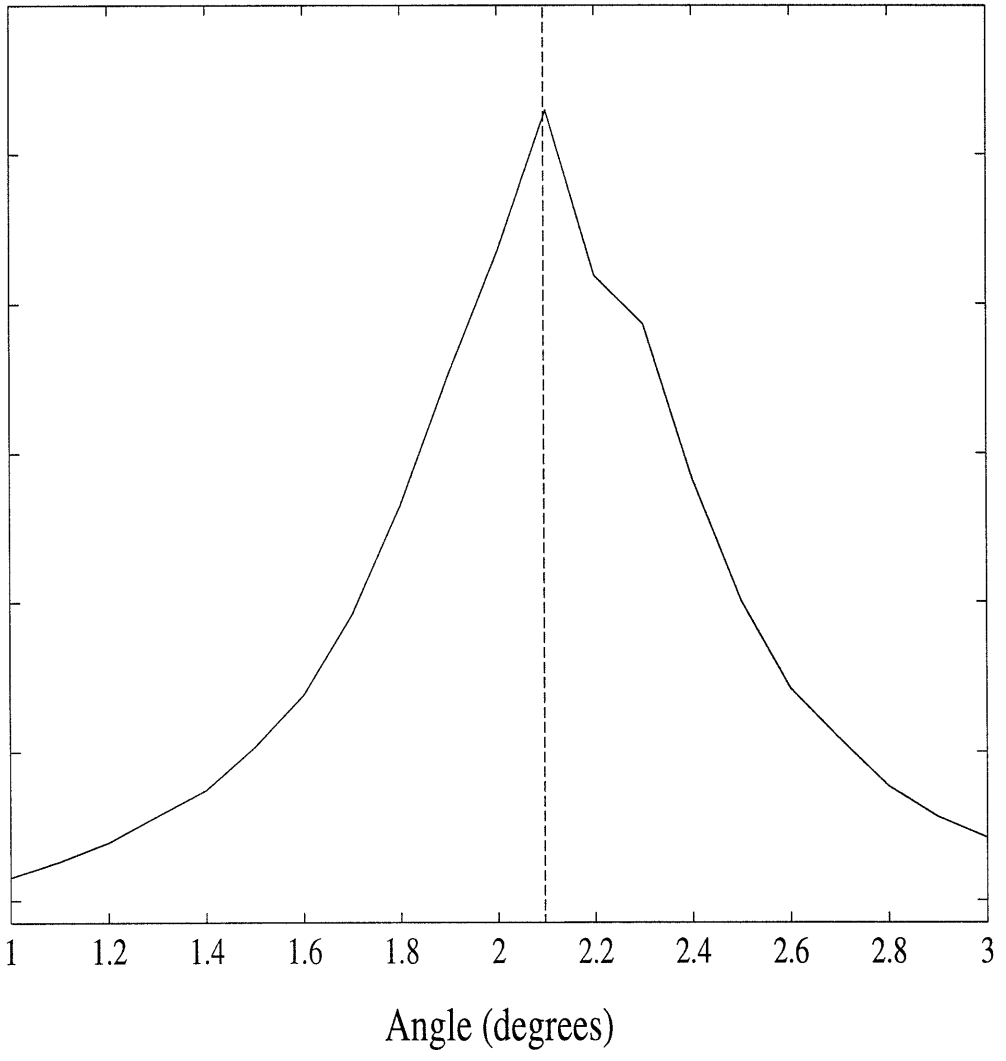

Figure 8: *Line angle estimate using the ESPRIT (dashed vertical line) and the Hough Transform (solid line) methods.*

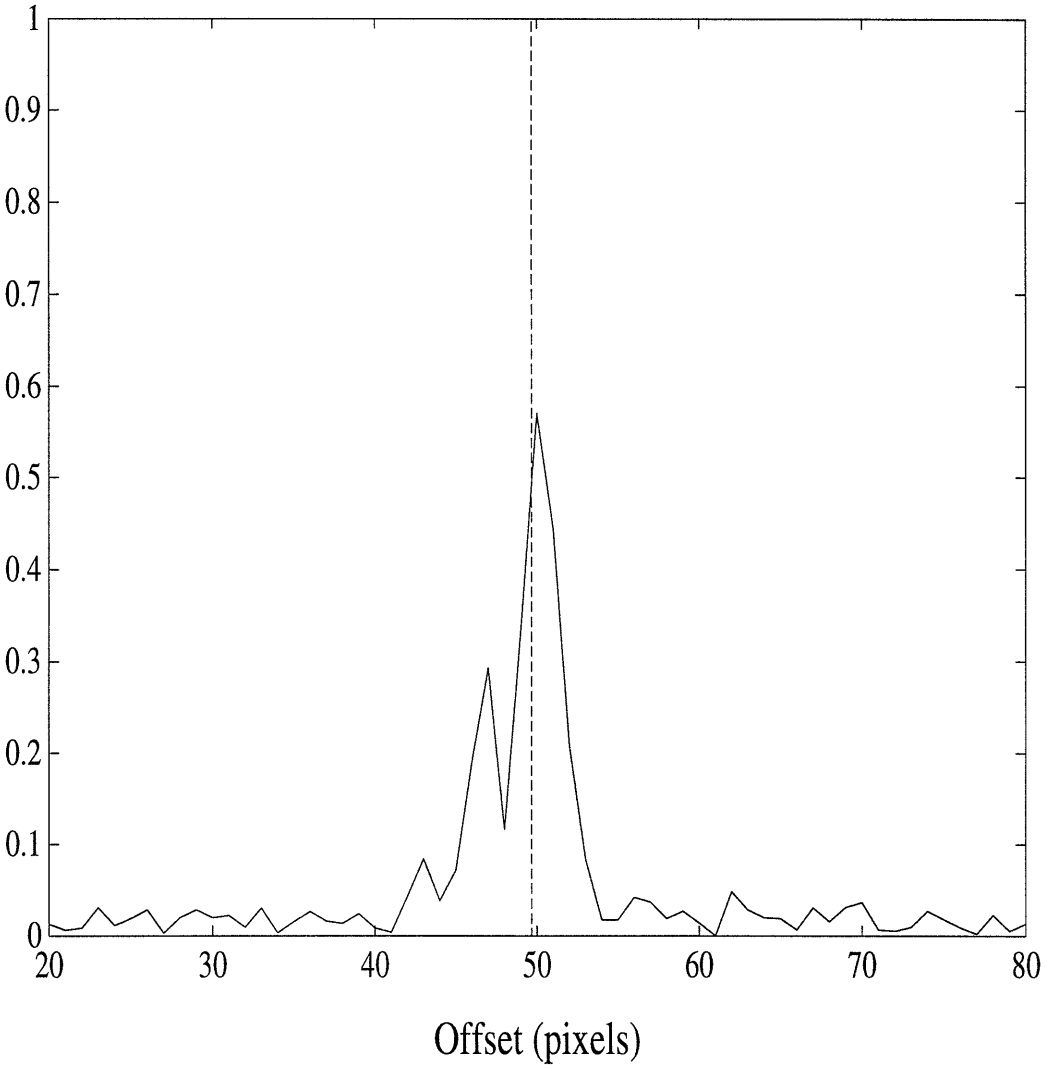

Figure 9: *Line offset estimate using the ESPRIT (dashed vertical line) and the Hough Transform (solid line) methods.*

7 Real Data Example

In this section, the viability of the various methods is tested on experimental radar data, provided by Professor S. Haykin of McMaster University. The receiver is an $L = 32$-element uniform linear array, which is mounted vertically so that the DOA is in this case the elevation angle. The sensors have a horizontal polarization. The array is located on the shore of a lake, whereas the transmitter is on the other side. Thus, the surface of the lake will ideally generate a specular multipath component. The orientation of the array is such that the direct and reflected waves impinge approximately symmetrically with respect to the broadside. Five data sets have been processed, in which the separation between the two signal paths (in electrical angles, see (28)) varies between $\Delta\phi = BW/5$ and $\Delta\phi = BW/3$, where $BW = 2\pi/L$ represents the standard beamwidth of the array (in radians).

The given five data sets were processed using the previously presented methods assuming a perfect ULA array response (28). In two of these data sets, none of the tested methods was able to locate two signal components in the vicinity of the postulated true values. In the other three sets, fairly good results were obtained. The results from two of the latter data sets are presented below. There are many possible reasons for the observed variability in the data. The most obvious is of course uncertainties in the receiving equipment, for example due to mutual coupling between sensor elements. The calibration requirements are generally quite high if one wants to achieve a resolution well within the beamwidth of the array. Other possible sources of errors are insufficient signal-to-noise ratio (SNR), spatial correlation of the noise field, etc. To illustrate the latter point, the eigenvalues of a typical sample covariance are depicted in Figure 10, along with a realization from the theoretical model. One should also bear in mind that in a real data experiment, there are actually no true values available for the estimated parameters. The postulated $\Delta\phi$ is calculated from the geometry of the experimental setup, but in practice the multipath component may very well be absent from some of the data sets, or it may impinge from an unexpected direction. In the following, the results from two successful data sets are presented. The sets are labeled A and B for reference. To obtain an idea of the statistical variability of the estimates, the data sets, each containing $N = 127$ snapshots, are first divided into 4 subsets of 32 samples (the last two subsets overlap by one snapshot). As a first attempt, the various spectral-based methods are applied. Since the signal components are expected to be highly correlated or even coherent, the spectral-based methods are likely to fail. However, the signals can be "de-correlated" by pre-processing the sample covariance matrix using forward-backward averaging (41). This has little or no effect on the beamforming techniques, but will be seen to improve the performance of the spectral-based subspace methods, particularly so for the Min-Norm method.

In Figure 11, the results from applying the traditional beamforming and the Capon methods to the 4 different A subsets are presented. The "spatial spectra" are all normalized such that the peak value is unity. The "true" DOAs (electrical angles, measured in fractions of the beamwidth) are indicated by vertical dotted lines in the plot. It is

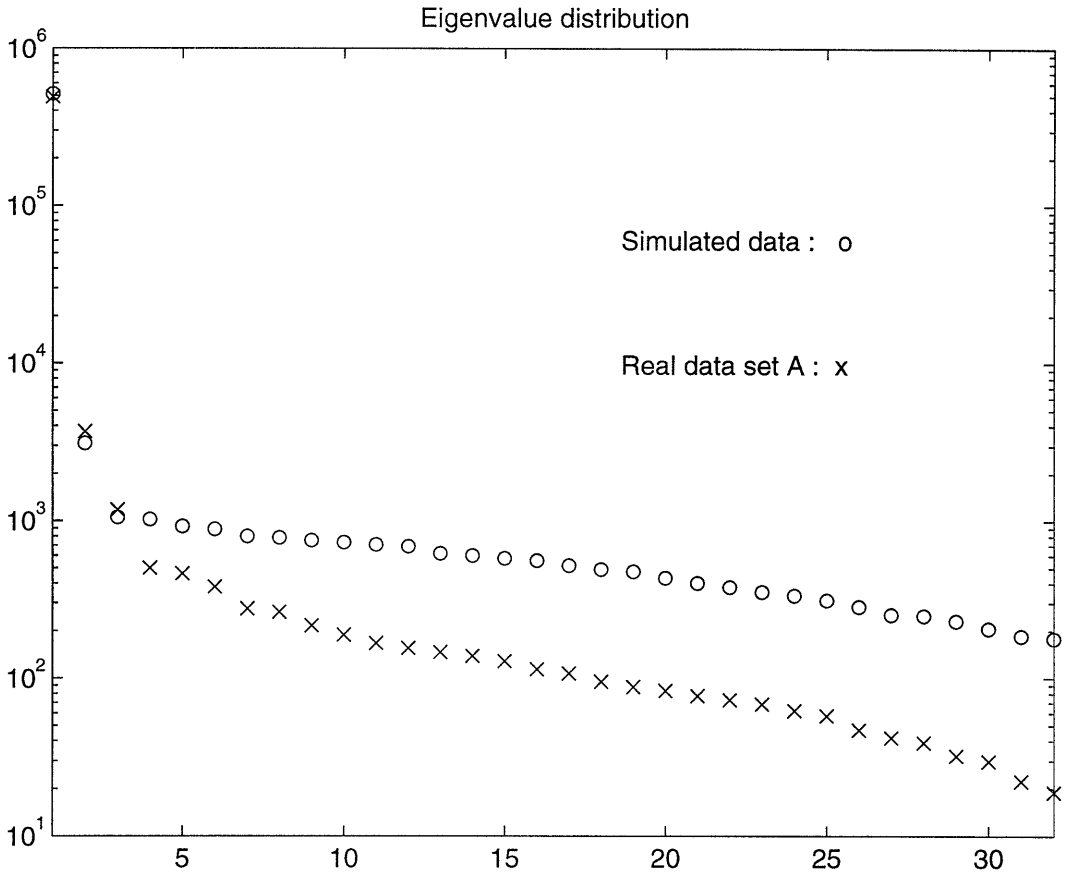

Figure 10: *Distribution of eigenvalues for 32-element uniform linear array. Simulated data and real data set A.*

clear that the beamforming methods fail to resolve the sources in this case. In Figure 12, the results for the MUSIC method with and without forward-backward averaging are shown. The presence of the two signal components is visible for the FB-MUSIC method, but the resolution capability is still not quite adequate. Finally, the Min-Norm method is applied and the resulting normalized "spatial spectra" are depicted in Figure 13. The Min-Norm method is known to have better resolution properties than MUSIC because of the inherent bias in the radii of the roots [55, 62], and using forward-backward averaging we see that Min-Norm performs satisfactorily in this scenario. Moving on to the parametric methods, we first apply the TLS ESPRIT method with forward-backward averaging and the WSF method. The results for both methods are excellent, as seen in Figure 14. The statistical variability appears to be smallest for the WSF method, as predicted by theory. The estimates from the SML and DML methods are virtually identical to those of

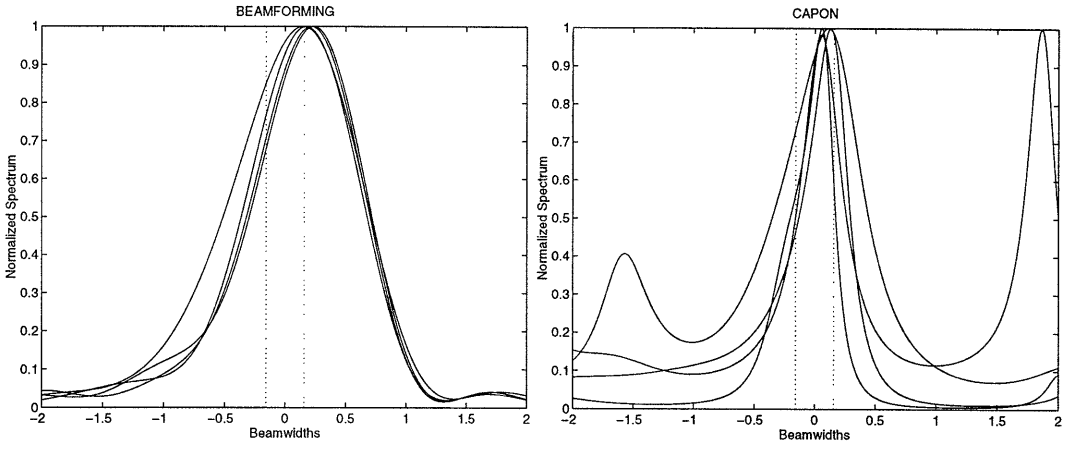

Figure 11: *Spatial spectra for the beamforming (left) and Capon (right) methods. The results from the 4 subsets of data set A are overlayed. The horizontal axis contains the electrical angle in fractions of the beamwidth. "True" DOAs indicated by vertical dotted lines.*

WSF for these data, and they are therefore not included in the plot. Finally, we applied the ESPRIT and WSF methods using all $N = 127$ snapshots from data set A, but with varying numbers of sensors. The results are shown in Figure 15. One can conclude that 23-25 sensors are required to resolve the signals in this data set. This corresponds to a source separation of about $\Delta\phi = 0.23$ beamwidths. The signal-to-noise ratio on data set A is estimated (using stochastic maximum likelihood) to SNR=15 dB for the signal at $\phi = 0.20$ and SNR=12 dB for the signal at $\phi = -0.20$. The signal correlation is estimated to

$$\rho_{12} = \frac{\mathrm{E}[s_1(t)s_2^*(t)]}{\sqrt{\mathrm{E}[|s_1(t)|^2]\,\mathrm{E}[|s_2(t)|^2]}} \approx 0.99\,e^{-2.95j} \ .$$

This clearly indicates a specular multipath component, since the signals are nearly coherent and have a phase difference close to 180°.

The corresponding numbers for data set B are SNR=6 dB for the signal at $\phi = 0.14$, SNR=2 dB for the signal at $\phi = -0.36$ (estimated locations) and

$$\rho_{12} \approx 0.99\,e^{-0.66j} \ .$$

Hence, data set B appears to be more noisy than set A, and the reflection in the lake appears to have caused a phase shift different from 180°. For this data set the postulated signal separation is smaller ($0.21\,BW$) than that of set A ($0.31\,BW$). The normalized "spatial spectra" for the Min-Norm method are shown in Figure 16. With forward-backward averaging, a second peak at about $-0.4\,BW$ is clearly visible. The TLS ESPRIT method did not produce satisfactory results on data set B, with or without forward-backward averaging. However, the more advanced parametric methods still appear to be useful.

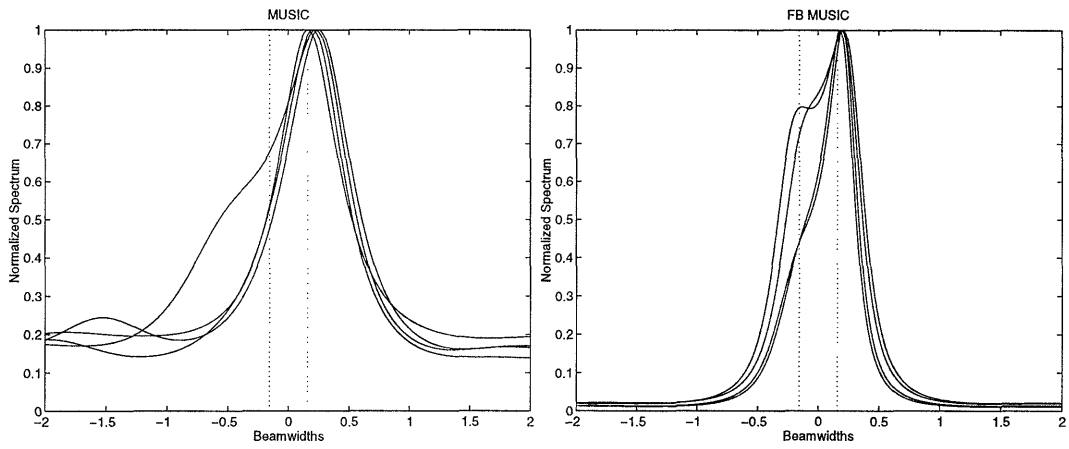

Figure 12: *Spatial spectrum for the MUSIC method, with (right) and without (left) forward-backward averaging.*

Again, the estimates from the WSF, SML and DML methods are virtually identical using all sensors, as seen in Figure 17. There is a rather clear trend in the estimates, and one might suspect non-stationary conditions during the data collection. Nevertheless, the different parametric methods were also applied using all $N = 127$ snapshots from data set B. In Figure 18, the estimates are plotted versus the number of sensors used by the algorithm. On these data, the estimates stabilize at about 26-28 sensors, corresponding to a source separation of about $\Delta\phi = 0.21$ beamwidths. However, as for the Min-Norm method there is a quite substantial bias in the estimate of the DOA at $\phi < 0$ (the multipath), assuming that the given "true DOAs" are correct. One could perhaps attribute this bias to the time-variations indicated in Figure 14.

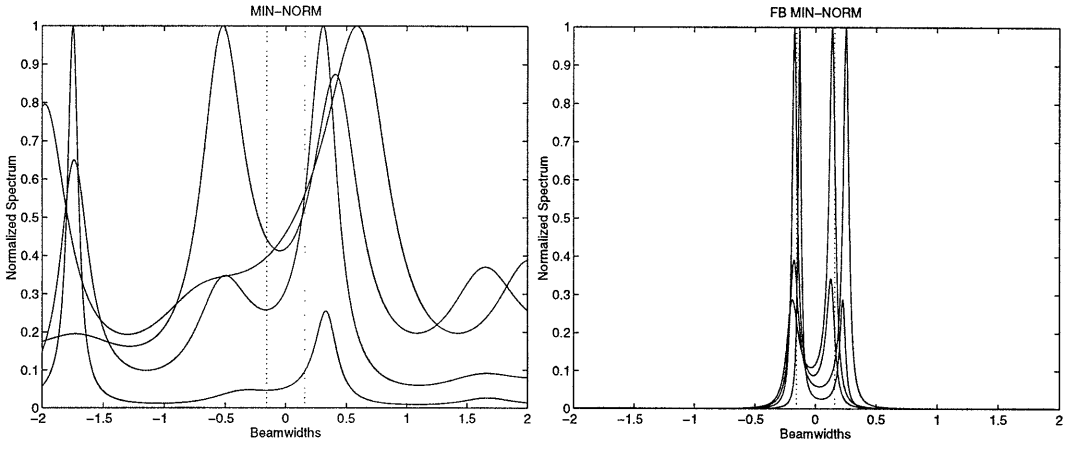

Figure 13: *Spatial spectrum for the Min-Norm method, with (right) and without (left) forward-backward averaging.*

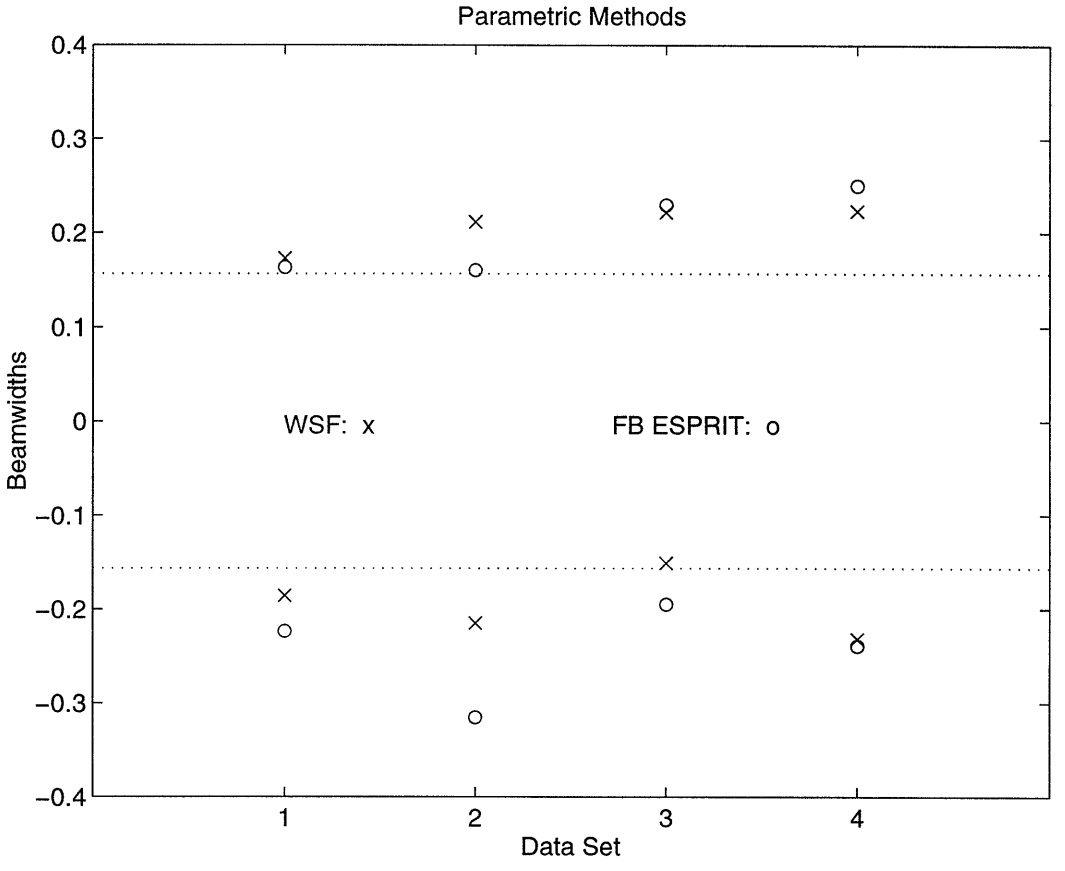

Figure 14: *Estimated electrical angles (in beamwidths) using the WSF and forward-backward TLS ESPRIT methods. The horizontal axis is the 4 different data subsets. "True" DOAs indicated by horizontal vertical lines.*

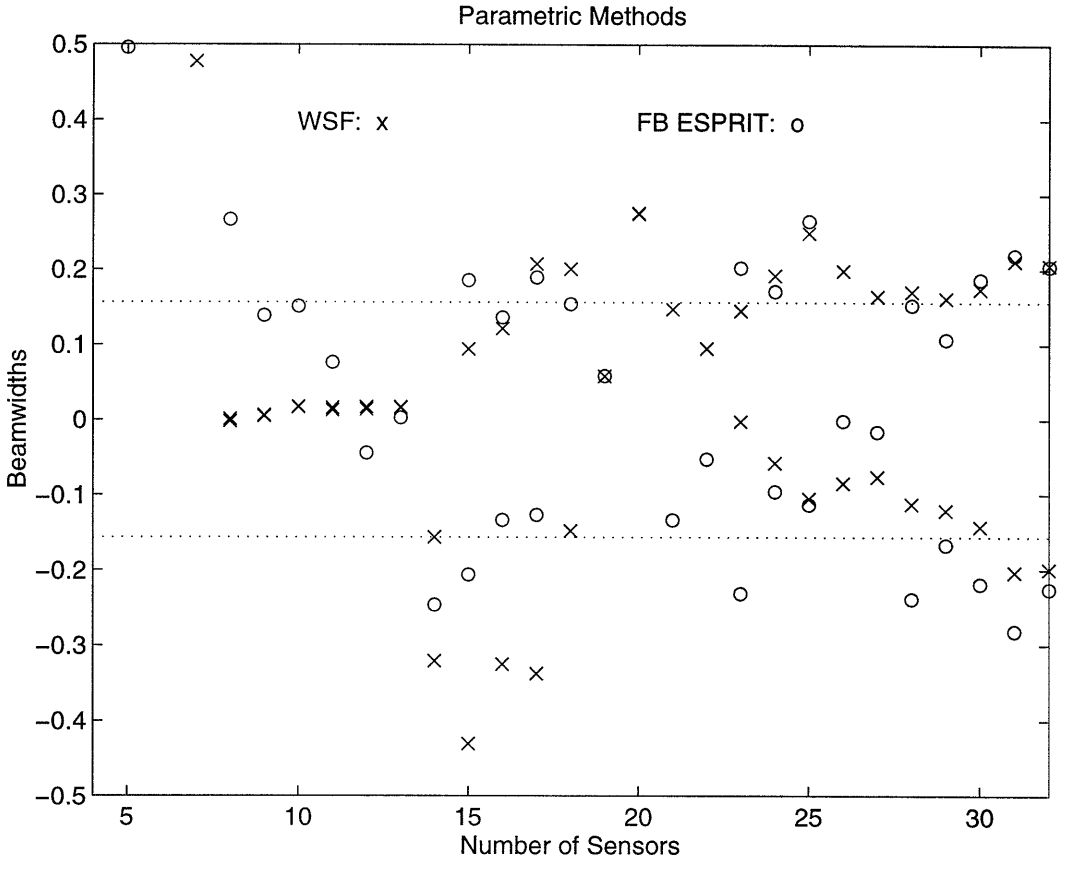

Figure 15: *Estimated electrical angles (in beamwidths) using the WSF and forward-backward TLS ESPRIT methods on the entire data set A. The horizontal axis is the number of sensors employed by the estimator. "True" DOAs indicated by horizontal vertical lines.*

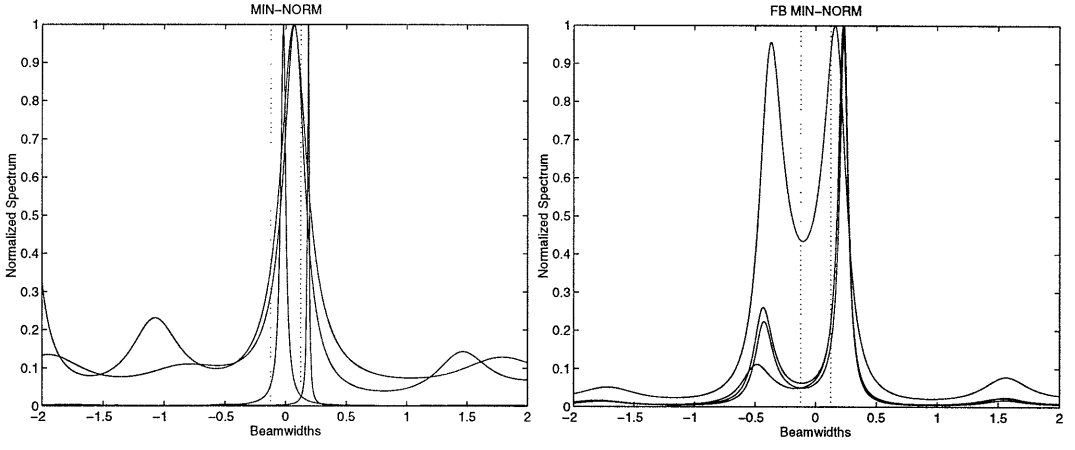

Figure 16: *Spatial spectrum for the Min-Norm method, with (right) and without (left) forward-backward averaging.*

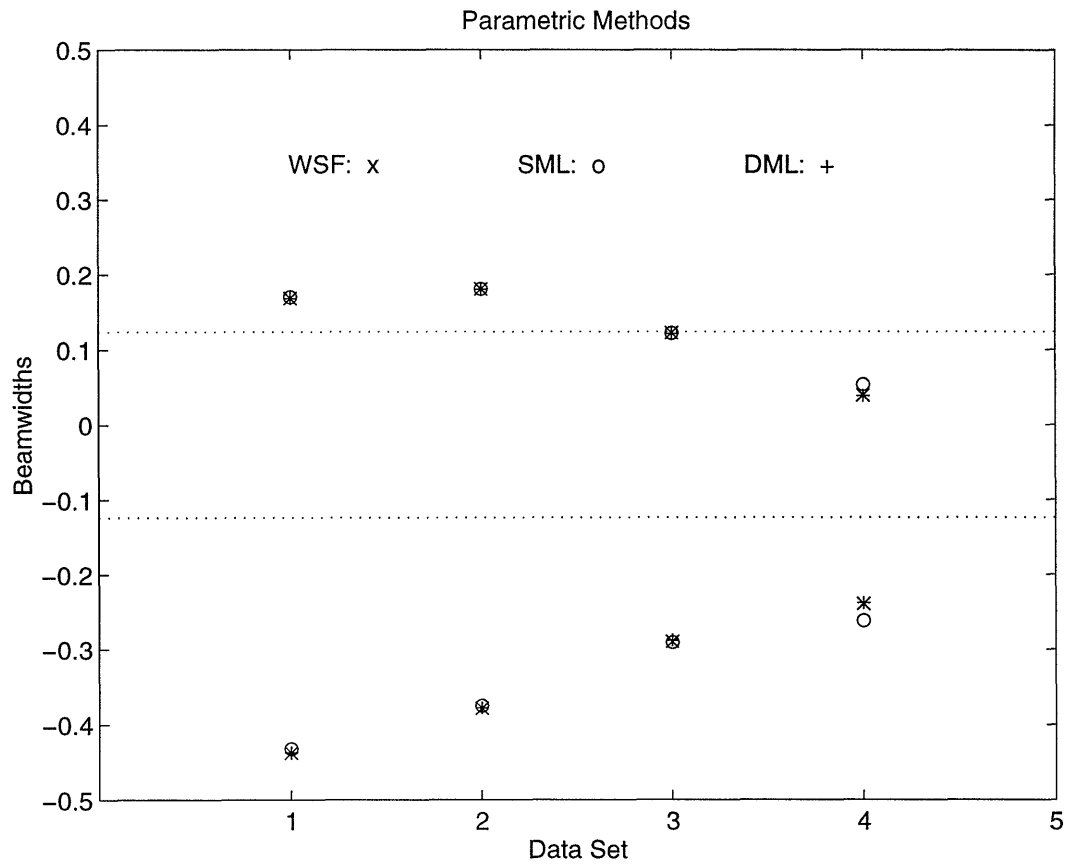

Figure 17: *Estimated electrical angles (in beamwidths) using the WSF, SML and DML methods. The horizontal axis is the 4 different data subsets. "True" DOAs indicated by horizontal vertical lines.*

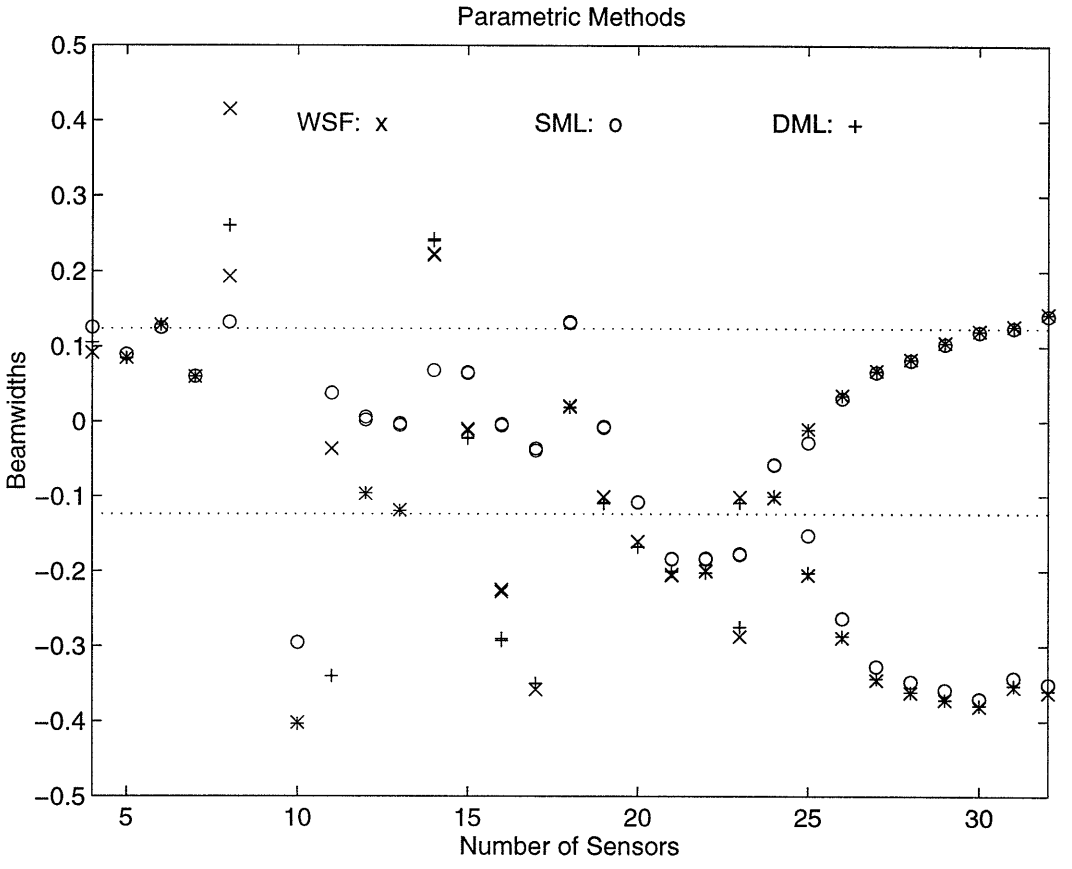

Figure 18: *Estimated electrical angles (in beamwidths) using the WSF, SML and DML methods on the entire data set B. The horizontal axis is the number of sensors employed by the estimator. "True" DOAs indicated by horizontal vertical lines.*

8 Conclusions

The depth acquired from the theoretical research in sensor array processing reviewed in this paper, have played a key role in helping identifying areas of applications. New real-world problems solvable using array signal processing techniques are regularly introduced, and it is expected that their importance will only grow as automatization becomes more widespread in industry, and as faster and cheaper digital processing system become available. This manuscript is not meant to be exhaustive, but rather as a broad review of the area, and more importantly as a guide for a first time exposure to an interested reader. The focus is on algorithms, whereas a deeper analysis and other more specialized research topics are only briefly touched upon.

In concluding the recent advances of the field, we think it is safe to say that the spectral-based subspace methods and, in particular, the more advanced parametric methods have clear performance improvements to offer as compared to beamforming methods. Resolution of closely spaced sources (within fractions of a beamwidth) have been demonstrated and documented in several experimental studies. However, high performance is not for free. The requirements on sensor and receiver calibration, mutual coupling, phase stability, dynamic range, etc. become increasingly more rigorous with higher performance specifications. Thus, in some applications the cost for achieving within-beamwidth resolution may still be prohibitive.

The quest for algorithms that perform well under ideal conditions and the understanding of their properties is in some sense over with the advances over the past years. However, the remaining work is not the less challenging, namely to adapt the teoretical methods to fit the particular demands in specific applications. For example, real-time requirements may place high demands on algorithm simplicity, and special array and signal structures present in certain scenarios must be exploited. The future work, also in academic research, will be much focused on bridging the gap that still exists between theoretical methods and real-world applications.

Acknowledgements

The authors are grateful to Professor S. Haykin of McMaster University for collecting the data used in Section 7, and to Professor M. Zoltowski of Purdue University for transfering the data. Thanks also to Dr. H. Aghajan of Stanford University for providing the figures of Section 6.3.

References

[1] B.G. Agee, A.V. Schell, and W.A. Gardner. "Spectral Self-Coherence Restoral: A New Approach to Blind Adaptive Signal Extraction Using Antenna Arrays". *Proc. IEEE*, 78:753–767, Apr. 1990.

[2] H.K. Aghajan and T. Kailath. Sensor Array Processing Techniques for Super Resolution Multi-Line-Fitting and Straight Edge Detection. *IEEE Trans. on Image Proc.*, 2(4), Oct. 1993.

[3] S. Anderson, M. Millnert, M. Viberg, and B. Wahlberg. An Adaptive Array for Mobile Communication Systems. *IEEE Trans. on veh. Tec.*, 40, 1991.

[4] T.W. Anderson. *An Introduction to Multivariate Statistical Analysis,* 2^{nd} *edition.* John Wiley & Sons, New York, 1984.

[5] S. Andersson. "Optimal Dimension Reduction for Sensor Array Signal Processing". *Signal Processing*, 30(2), Jan. 1993.

[6] S.P. Applebaum. Adaptive Arrays. *IEEE Trans. Antennas and Propagation*, 24(9):585–598, Sept. 1976.

[7] Articles. Spectra From Various Techniques. *IEEE Proceedings*, 69(11), 1981. Special Issue.

[8] Articles. Time Delay Estimation. *IEEE Trans. on Acoustics, Speech and Signal Proc.*, ASSP-29(3), June 1981. Special Issue.

[9] Articles. Spectral Estimation. *IEEE Proceedings*, 70(9), 1982. Special Issue.

[10] A.B. Baggeroer, W.A. Kuperman, and H. Schmidt. Matched field processing:Source localization in correlated noise as an optimum parameter estimation problem. *J. Acoust. Soc. Am.*, 83(2):571–587, February 1988.

[11] A.J. Barabell. "Improving the Resolution Performance of Eigenstructure-Based Direction-Finding Algorithms". In *Proc. ICASSP 83*, pages 336–339, Boston, MA, 1983.

[12] G. Bienvenu and L. Kopp. Adaptivity to background Noise spatial coherence for high resolution passive methods. In *Int. Conf. on Acoust., Speech and Signal Processing*, pages 307–310, 1980.

[13] G. Bienvenu and L. Kopp. Méthodes Haute Resolution Apres Formation de Voies. In *Conference du GRETSI*, volume 1, pages 325–330, Nice, France, May 1985.

[14] J.F. Böhme. "Estimation of Source Parameters by Maximum Likelihood and Nonlinear Regression". In *Proc. ICASSP 84*, pages 7.3.1–7.3.4, 1984.

[15] J.F. Böhme. "Estimation of Spectral Parameters of Correlated Signals in Wavefields". *Signal Processing*, 10:329–337, 1986.

[16] J.F. Böhme and D. Kraus. "On Least Squares Methods for Direction of Arrival Estimation in the Presence of Unknown Noise Fields". In *Proc. ICASSP 88*, pages 2833–2836, New York, N.Y., 1988.

[17] Y. Bresler and A. Macovski. "Exact Maximum Likelihood Parameter Estimation of Superimposed Exponential Signals in Noise". *IEEE Trans. ASSP*, ASSP-34:1081–1089, Oct. 1986.

[18] Y. Bresler and A. Macovski. "On the Number of Signals Resolvable by a Uniform Linear Array". *IEEE Trans. ASSP*, ASSP-34:1361–1375, Oct. 1986.

[19] K. Buckley and X.-L. Xu. "Spatial-spectrum estimation in a location sector". *IEEE Trans. ASSP*, 38:1842–1852, Nov. 1990.

[20] K.M Buckley and L.J. Griffiths. An Adaptive Generalized Sidelobe Canceller with Derivative Constraints. *IEEE Trans. on Antennas and Propagation*, AP-34(3):3111–319, 1986 1986.

[21] J. Burg. Maximum entropy spectral analysis. In *37th Meeting Society Exploration Geophysicists*, 1967.

[22] J.A. Cadzow. "Multiple Source Location-The Signal Subspace Approach". *IEEE Trans. ASSP*, ASSP-38:1110–1125, July 1990.

[23] J. Capon. High-Resolution frequency-wavenumber spectrum analysis. *Proc. IEEE*, 57(8):2408–1418, Aug. 1969.

[24] Y.-H. Chen and Y.-S. Lin. "DOA estimation by fourth-order cumulants in unknown noise environments". In *Proc. IEEE ICASSP*, volume 4, pages 296–299, Minneapolis, MN, Apr. 1993.

[25] H. Clergeot, S. Tressens, and A. Ouamri. "Performance of High Resolution Frequencies Estimation Methods Compared to the Cramér-Rao Bounds". *IEEE Trans. ASSP*, 37(11):1703–1720, November 1989.

[26] P. Comon and G. H. Golub. "Tracking a few Extreme Singular Values and Vectors in Signal Processing". *Proceedings of the IEEE*, 78:1327–1343, Aug. 1990.

[27] J.H. Cozzens and M.J. Sousa. Source Enumeration in a Correlated Signal Environment. *IEEE Trans. on Acoust., Speech and Signal Proc.*, 42(2):304–317, Feb. 1994.

[28] R. DeGroat. "Noniterative subspace tracking". *IEEE Trans on SP*, 40(3):571–577, 1992.

[29] A. Di. Multiple source location-a matrix decomposition approach. *IEEE Trans. on Acoustics, Speech and Signal Processing*, ASSP-33:1086–1091, Oct. 1985.

[30] S. Haykin (ed.). *Array Signal Processing.* Prentice-Hall, Englewood Cliffs, NJ, 1985.

[31] J. E. Evans, J. R. Johnson, and D. F. Sun. Application of Advanced Signal Processing Techniques to Angle of Arrival Estimation in ATC Navigation and Surveillance Systems. Technical report, MIT Lincoln Laboratory, June 1982.

[32] A. Farina. *Antenna-Based Signal Processing Techniques for Radar Systems.* Artech House, Norwood, MA, 1992.

[33] D.R. Farrier and L.R. Prosper. "A Signal Subspace Beamformer". In *Proc. ICASSP 90*, pages 2815–2818, Albuquerque, NM, 1990.

[34] A.J. Fenn, C.J. Diederich, and P.R. Stauffer. An Adaptive-Focusing Algorithm for a Microwave Planar Phased-Array Hyperthermia System. *The Lincoln Laboratory Journal*, 6(2):269–288, 1993.

[35] A.J. Fenn and G.A. King. "Adaptive Nulling in the Hyperthermia Treatment of Cancer. *The Lincoln Laboratory Journal*, 5(2):223–240, 1992.

[36] A.J. Fenn and G.A. King. Adaptive radio-frequency hyperthermia-phased array system for improved cancer therapy: phantom target measurements. *International Journal of Hyperthermia*, 10(2):189–208, March-April 1994.

[37] P. Forster. *Méthodes De Traitement d'Antenne Aprés Filtrage Spatial.* PhD thesis, Université de Rennes, France, 1988.

[38] P. Forster and G. Vezzosi. "Application of Spheroidal Sequences to Array Processing". In *Proc. ICASSP 87*, pages 2268–2271, Dallas, TX, 1987.

[39] B. Friedlander. "Sensitivity Analysis of the Maximum Likelihood Direction-Finding Algorithm". *IEEE Trans. AES*, AES-26(6):953–968, Nov. 1990.

[40] B. Friedlander and A. Weiss. "Direction Finding Using Spatial Smoothing with Interpolated Arrays". *IEEE Trans. AES*, 28:574–587, Apr. 1992.

[41] O.L. Frost. An Algorithm for Linearly Constrained Adaptive Array Processing. *Proc. of the IEEE*, 60(8):926–935, August 1972.

[42] W.F. Gabriel. Spectral Analysis and Adaptive Array Superresolution Techniques. *Proceedings of the IEEE*, 68(6):654–666, June 1980.

[43] G.H. Golub and C.F. VanLoan. "An Analysis of the Total Least Squares Problem". *SIAM J. Num. Anal.*, 17:883–893, 1980.

[44] G.H. Golub and C.F. VanLoan. *Matrix Computations, 2nd edition.* Johns Hopkins University Press, Baltimore, MD., 1989.

[45] R.P. Gooch and J. Lundel. "The CM Array: An Adaptive Beamformer for Constant Modulus Signals". In *Proc. ICASSP 86*, pages 2523–2526, Tokyo, Japan, 1986.

[46] N. Härle and J.F. Böhme. Detection of knocking for Spark Ignition Engines based on StructuralVibrations. In *Int. Conf. on Acoust., Speech and Signal Processing*, pages 1744–1747, 1987.

[47] S. Haykin. Radar array processing for angle of arrival estimation. In S. Haykin, editor, *Array Signal Processing.* Prentice-Hall, Englewood Cliffs, NJ, 1985.

[48] S. Haykin, J. Litva, and T.J. Shepherd (eds). *Radar Array Processing.* Springer-Verlag, Berlin, 1993.

[49] Harold Hotelling. "Analysis of a Complex of Statistical Variables into Principal Components". *J. Educ. Psych.*, 24:417–441,498–520, 1933.

[50] H. Hung and M. Kaveh. "Focussing Matrices for Coherent Signal-Subspace Processing". *IEEE Trans. ASSP*, ASSP-36:1272–1281, Aug. 1988.

[51] A. G. Jaffer. "Maximum Likelihood Direction Finding of Stochastic Sources: A Separable Solution". In *Proc. ICASSP 88*, volume 5, pages 2893–2896, New York, New York, April 1988.

[52] Don H. Johnson and Dan E. Dudgeon. *Array Signal Processing - Concepts and Techniques.* Prentice-Hall, Englewood Cliffs, NJ, 1993.

[53] E. C. Jordan and K. G. Balman. *Electromagnetic Waves and Radiating Systems.* Prentice-Hall, New Jersey, second edition edition, 1968.

[54] I. Karasalo. "Estimating the Covariance Matrix by Signal Subspace Averaging ". *IEEE Trans. ASSP*, ASSP-34(1):8–12, February 1986.

[55] M. Kaveh and A. J. Barabell. "The Statistical Performance of the MUSIC and the Minimum-Norm Algorithms in Resolving Plane Waves in Noise". *IEEE Trans. ASSP*, ASSP-34:331–341, April 1986.

[56] M. Kaveh and A. Bassias. "Threshold extension based on a new paradigm for MUSIC-type estimation". In *Proc. ICASSP 90*, pages 2535–2538, Albuquerque, NM, April 1990.

[57] S.M. Kay and V. Nagesha. "Maximum Likelihood Estimation of Signals in Autoregressive Noise". *IEEE Trans on SP*, 42:88–101, Jan. 1994.

[58] T. Koopmans. *Linear Regression Analysis of Economic Time Series.* Haarlem, De Erven F. Bohn N.V., 1937.

[59] D. Kraus and J.F. Böhme. "Maximum likelihood location estimation of wideband sources using the EM algorithm". In *Adapt. Syst. in Contr. and Sig. Proc. 1992. Selected Papers from the 4th IFAC Symposium*, pages 487–491, Grenoble, France, 1993.

[60] H. Krim. *Detection and Parameter Estimation of Correlated Signals in Noise.* PhD thesis, North. Univ., June 1991.

[61] H. Krim. A Data-Based Enumeration of Fully Correlated Signals. *IEEE Trans. Acoust., Speech, Signal Processing*, July 1994.

[62] H. Krim, P. Forster, and J. G. Proakis. Operator Approach To Performance Analysis Of Root-MUSIC and Root Min-Norm. *IEEE Trans. Acoust., Speech, Signal Processing*, July 1992.

[63] H. Krim and J. G. Proakis. Smoothed eigenspace-based paramerter estimation. *Automatica, Special Issue on Statistical Signal Procssing and Control*, Jan. 1994.

[64] R. Kumaresan and D. W. Tufts. Estimating the Angles of Arrival of Multiple Plane Waves. *IEEE Trans. on Aeros. and Elect. Sys.*, AES-19(1), January 1983.

[65] S.Y. Kung. "A New Identification and Model Reduction Algorithm via Singular Value Decomposition". In *Proc. 12th Asilomar Conf. on Circuits, Systems and Computers*, pages 705–714, Pacific Grove, CA, November 1978.

[66] F. Li, J. Vaccaro, and D. W. Tufts. Min-Norm Linear Prediction For Arbitrary Sensor Arrays. In *Int. Conf. on Acoust., Speech and Signal Processing*, pages 2613–2616, 1989.

[67] F. Li and R. Vaccaro. "Sensitivity Analysis of DOA Estimation Algorithms to Sensor Errors". *IEEE Trans. AES*, AES-28(3):708–717, July 1992.

[68] F. Li and R.J. Vaccaro. "Performance Degradation of DOA Estimators Due to Unknown Noise Fields". *IEEE Trans. SP*, SP-40(3):686–689, March 1992.

[69] W.S. Liggett. *Passive Sonar: Fitting Models to Multiple Time Series*, volume Signal Processing, pages 327–345. Academic Press, New York, j.w.r. griffiths and p.l. stocklin and c. vam schoonefeld edition, 1973.

[70] H. Liu, G. Xu, and L. Tong. A deterministic approach to blind equalization. In *Proc. of Asilomar*, pages 751–755, Monterey, Nov. 1993.

[71] C.P. Mathews and M. D. Zoltowski. "Eigenstructure techniques for 2-D angle estimation with uniform circular arrays". *IEEE Trans. on SP*, 42:2395–2407, Sept. 1994.

[72] P. Milanfar. *Geometric Estimation and Reconstruction from Tomographic Data.* PhD thesis, MIT, Cambridge, MA, 1993.

[73] P. Milanfar, G.C. Verghese, W.C. Karl, and A.S. Willsky. Reconstructing Polygons from Moments with Connections to Array Processing. *IEEE Trans. on Signal Proc.*, To Appear.

[74] J.S. Mosher, R.M. Leahy, and P.S. Kewis. "Biomagnetic localization from transient quasi-static events". In *Proc. ICASSP 93*, volume 1, pages 91–94, Minneapolis, MN, 1993.

[75] B. Ottersten and T. Kailath. "Direction-of-Arrival Estimation for Wide-Band Signals Using the ESPRIT Algorithm". *IEEE Trans. ASSP*, ASSP-38(2):317–327, Feb. 1990.

[76] B. Ottersten, M. Viberg, and T. Kailath. "Analysis of Subspace Fitting and ML Techniques for Parameter Estimation from Sensor Array Data". *IEEE Trans. on SP*, SP-40:590–600, March 1992.

[77] B. Ottersten, M. Viberg, P. Stoica, and A. Nehorai. Exact and large sample ML techniques for parameter estimation and detection in array processing. In Haykin, Litva, and Shepherd, editors, *Radar Array Processing*, pages 99–151. Springer-Verlag, Berlin, 1993.

[78] N.L. Owsley. *SONAR ARRAY PROCESSING*, chapter 3, pages 115–184. Haykin, Editor. Prentice Hall, Englewood Cliffs, New Jersey, 1985.

[79] A. Paulraj and T. Kailath. "Eigenstructure Methods for Direction-of-Arrival Estimation in the Presence of Unknown Noise Fields". *IEEE Trans. on ASSP*, ASSP-33:806–811, Aug. 1985.

[80] A. Paulraj, R. Roy, and T. Kailath. "A Subspace Rotation Approach to Signal Parameter Estimation". *Proceedings of the IEEE*, pages 1044–1045, July 1986.

[81] V.F. Pisarenko. "The retrieval of harmonics from a covariance function". *Geophys. J. Roy. Astron. Soc.*, 33:347–366, 1973.

[82] B. Porat and B. Friedlander. "Direction Finding Algorithms Based on High-Order Statistics". *IEEE Trans. SP*, SP-39:2016–2024, Sept. 1991.

[83] J.G. Proakis and D.G. Manolakis. *Digital Signal Processing, second edition.* Macmillan, New York, 1992.

[84] B. D. Rao and K. V. S. Hari. Performance analysis of ESPRIT and TAM in determining the direction of arrival of plane waves in noise. *IEEE Trans. ASSP*, ASSP-37(12):1990–1995, Dec. 1989.

[85] B. D. Rao and K.V.S. Hari. Performance Analysis of Root-MUSIC. *IEEE Trans. Acoust., Speech, Signal Processing*, 37(12):1939–1949, December 1989.

[86] Y. Rockah and P. M. Schultheiss. Array shape calibration using sources in unknown locations – Part I: Far-field sources. *IEEE Trans. on ASSP*, 35:286–299, March 1987.

[87] R. Roy and T. Kailath. "ESPRIT – Estimation of Signal Parameters via Rotational Invariance Techniques". *IEEE Trans. on ASSP*, ASSP-37(7):984–995, July 1989.

[88] Jr. R.T. Compton. *Adaptive Antennas.* Prentice Hall, Englewood Cliffs, NJ, 1988.

[89] S. Sakagami, S. Aoyama, K. Kuboi, S. Shirota, and A. Akeyama. "Vehicle Position Estimates by Multibeam Antennas in Multipath Environments". *IEEE Trans. on Vehicular Tech.*, 41(1):63–68, Feb. 1992.

[90] S.V. Schell and W.A. Gardner. "Blind adaptive spatiotemporal filtering for wide-band cyclostationary signals". *IEEE Trans. SP*, 41:1961–1964, May 1993.

[91] R. O. Schmidt. *A Signal Subspace Approach to Multiple Emitter Location and Spectral Estimation.* PhD thesis, Stanford Univ., Stanford, CA, Nov. 1981.

[92] S. Shamsunder and G. Giannakis. "Signal selective localization of nonGaussian cyclostationary sources". *IEEE Trans. SP*, 42:2860–2864, Oct. 1994.

[93] T. J. Shan, M. Wax, and T. Kailath. On spatial smoothing for directions of arrival estimation of coherent signals. *IEEE Trans. on Acoustics, Speech and Signal Processing*, ASSp-33(4):806–811, April 1985.

[94] S. Sivanand, J.-F. Yang, and M. Kaveh. "Focusing filters for wide-band direction finding". *IEEE Trans. SP*, 39:437–445, Feb. 1991.

[95] D.T.M. Slock. "Blind Fractionally-Spaced Equalization, Perfect-Reconstruction Filter Banks and Multichannel Linear Prediction". In *Proc. ICASSP 94*, volume 4, pages 585–588, Adelaide, Australia, April 1994.

[96] K. Steiglitz and L. McBride. "A technique for identification of linear systems". *IEEE Trans. Autom. Contr.*, AC-10:461–464, Oct. 1965.

[97] P. Stoica and A. Nehorai. "MUSIC, Maximum Likelihood and Cramér-Rao Bound". *IEEE Trans. ASSP*, ASSP-37:720–741, May 1989.

[98] P. Stoica and A. Nehorai. "MODE, Maximum Likelihood and Cramér-Rao Bound: Conditional and Unconditional Results". In *Proc. ICASSP 90 Conf*, pages 2715–2718, Albuquerque, NM, April 1990.

[99] P. Stoica and A. Nehorai. "MUSIC, Maximum Likelihood and Cramér-Rao Bound: Further Results and Comparisons". *IEEE Trans. ASSP*, ASSP-38:2140–2150, December 1990.

[100] P. Stoica and A. Nehorai. "Performance Study of Conditional and Unconditional Direction-of-Arrival Estimation". *IEEE Trans. ASSP*, ASSP-38:1783–1795, October 1990.

[101] P. Stoica and K. Sharman. "A Novel Eigenanalysis Method for Direction Estimation". *Proc. IEE*, F:19–26, Feb 1990.

[102] P. Stoica and K. Sharman. "Maximum Likelihood Methods for Direction-of-Arrival Estimation". *IEEE Trans. ASSP*, ASSP-38:1132–1143, July 1990.

[103] P. Stoica and T. Söderström. "Statistical Analysis of MUSIC and Subspace Rotation Estimates of Sinusoidal Frequencies". *IEEE Trans. ASSP*, ASSP-39:1836–1847, Aug. 1991.

[104] P. Stoica, M. Viberg, and B. Ottersten. "Instrumental Variable Approach to Array Processing in Spatially Correlated Noise Fields". *IEEE Trans. SP*, SP-42:121–133, Jan. 1994.

[105] M. Stojanovic and Z. Zvonar. Adaptive spatial/temporal multiuser receivers for time-varying channels with severe isi. In *Proc. of Conf. on Signals and Systems*, Princeton, March 1994.

[106] G. Su and M. Morf. "Modal Decomposition Signal Subspace Algorithms". *IEEE Trans. ASSP*, ASSP-34(3):585–602, June 1986.

[107] S.C. Swales, M.A. Beach, and D.J. Edwards. "Multi-Beam Adaptive Base Station Antennas for Cellular Land Mobile Radio Systems". In *Proc. IEEE Veh. Technol. Conf.*, pages 341–348, 1989.

[108] A. Swindlehurst and T. Kailath. "A Performance Analysis of Subspace-Based Methods in the Presence of Model Errors - Part I: The MUSIC Algorithm". *IEEE Trans. SP*, SP-40(7):1758–1774, July 1992.

[109] A. Swindlehurst and T. Kailath. "A Performance Analysis of Subspace-Based Methods in the Presence of Model Errors: Part 2 – Multidimensional Algorithms". *IEEE Trans. on SP*, SP-41:2882–2890, Sept. 1993.

[110] S. Talwar, M. Viberg, and A. Paulraj. "Estimating Multiple Co-Channel Digital Signals Using an Antenna Array". *IEEE SP Letters*, 1:29–31, Feb. 1994.

[111] L. Tong, G. Xu, and T. Kailath. "A New Approach to Blind Identification and Equalization of Multipath Channels". *IEEE Trans. on Inf. Theory*, To appear.

[112] H. L. Van Trees. *Detection, Estimation and Modulation Theory, part. I.* J. Wiley & Sons Inc., 1968.

[113] D. W. Tufts and R. Kumaresan. Estimation of frequencies of multiple Sinusoids: Making Linear Prediction Perform Like Maximum Likelihood. *IEEE Proceedings*, 70(9), September 1982.

[114] F. Tuteur and Y. Rockah. "A New Method for Detection and Estimation Using the Eigenstructure of the Covariance Difference". In *Proc. ICASSP 88 Conf*, pages 2811–2814, Tokyo, Japan, 1986.

[115] B.D. VanVeen and K.M. Buckley. Beamforming:A Versatile Approach to Spatial Filtering. *Signal Proc. Magazine*, pages 4–24, April 1988.

[116] B.D. Van Veen and B. Williams. "Dimensionality Reduction in High Resolution Direction of Arrival Estimation". In *Proc. Asilomar Conf. Sig., Syst., Comput.*, Pacific Groove, CA, Oct. 1988.

[117] M. Viberg and B. Ottersten. "Sensor Array Processing Based on Subspace Fitting". *IEEE Trans. SP*, SP-39(5):1110–1121, May 1991.

[118] M. Viberg, B. Ottersten, and T. Kailath. "Detection and Estimation in Sensor Arrays Using Weighted Subspace Fitting". *IEEE Trans. SP*, SP-39(11):2436–2449, Nov. 1991.

[119] M. Viberg and A.L. Swindlehurst. "A Bayesian Approach to Auto-Calibration for Parametric Array Signal Processing". *IEEE Trans. SP*, 42, Dec. 1994.

[120] M. Viberg and A.L. Swindlehurst. "Analysis of the Combined Effects of Finite Samples and Model Errors on Array Processing Performance". *IEEE Trans. SP*, 42:3073–3083, Nov. 1994.

[121] Mats Viberg. "Sensitivity of Parametric Direction Finding to Colored Noise Fields and Undermodeling". *Signal Processing*, 34(2):207–222, Nov. 1993.

[122] M. Wax. *Detection and Estimation of Superimposed Signals.* PhD thesis, Stanford Univ., Stanford, CA, March 1985.

[123] M. Wax. "Detection and Localization of Multiple Sources in Noise with Unknown Covariance". *IEEE Trans. on ASSP*, ASSP-40(1):245–249, Jan. 1992.

[124] M. Wax and T. Kailath. Detection of Signals by Information Theoretic Criteria. *IEEE Trans. on Acoustics, Speech and Signal Processing*, ASSP-33(2):387–392, February 1985.

[125] M. Wax, T.J. Shan, and T. Kailath. "Spatio-Temporal Spectral Analysis by Eigenstructure Methods". *IEEE Trans. ASSP*, ASSP-32, Aug. 1984.

[126] M. Wax and I. Ziskind. "On Unique Localization of Multiple Sources by Passive Sensor Arrays". *IEEE Trans. on ASSP*, ASSP-37(7):996–1000, July 1989.

[127] A. J. Weiss and B. Friedlander. "Array Shape Calibration Using Sources in Unknown Locations - A Maximum Likelihood Approach". *IEEE Trans. on ASSP*, 37(12):1958–1966, Dec. 1989.

[128] B. Widrow, K. M. Duvall, R. P. Gooch, and W. C. Newman. Signal Cancellation Phenomena in Adaptive Antennas: Causes and Cures. *IEEE Trans. Antennas and Propagation*, AP-30(5):469–478, July 1982.

[129] N. Wiener. *Extrapolation, Interpolation and Smoothing of Stationary Time Series.* MIT Press, Cambridge, MA, 1949.

[130] J.H. Winters. "Optimum combining for indoor radio systems with multiple users". *IEEE Trans. Communications*, 35:1222–1230, 1987.

[131] K.M. Wong, J.P. Reilly, Q. Wu, and S. Qiao. "Estimation of the Directions of Arrival of Signals in Unknown Correlated Noise, Parts I and II". *IEEE Trans. on SP*, SP-40:2007–2028, Aug. 1992.

[132] Q. Wu and K.M. Wong. "UN-MUSIC and UN-CLE: An Application of Generalized Canonical Correlation Analysis to the Estimation of the Directions of Arrival". *IEEE Trans. SP*, 42, Sept. 1994.

[133] G. Xu and T. Kailath. "Direction-of-arrival estimation via exploitation of cyclostationary-a combination of temporal and spatial processing". *IEEE Trans. SP*, 40(7):1775–1786, July 1992.

[134] G. Xu and T. Kailath. "Fast Subspace Decomposition". *IEEE Trans. SP*, 42(3):539–551, March 1994.

[135] W. Xu and M. Kaveh. "Design of signal-subspace cost functionals for parameter estimation". In *Proc. ICASSP 92*, volume 5, pages 405–408, San Francisco, CA, Mar. 1992.

[136] W. Xu, J. Pierre, and M. Kaveh. "Practical detection with calibrated arrays". In *Proc. 6:th SP Workshop on Statistical Signal and Array Processing*, pages 82–85, Victoria, Canada, Oct. 1992.

[137] X.-L. Xu and K. Buckley. "Bias analysis of the MUSIC location estimator". *IEEE Trans. SP*, 40(10):2559–2569, Oct. 1992.

[138] X.-L. Xu and K. Buckley. "An analysis of beam-space source localization". *IEEE Trans. SP*, 41(1):501–504, Jan. 1993.

[139] J.-F. Yang and M. Kaveh. "Adaptive eigensubspace algorithms for direction or frequency estimation and tracking". *IEEE Trans. ASSP*, 36(2):241–251, Feb. 1988.

[140] L.C. Zhao, P.R. Krishnaiah, and Z.D. Bai. "On Detection of the Number of Signals in Presence of White Noise". *J. of Multivariate Analysis*, 20:1:1–25, 1986.

[141] I. Ziskind and M. Wax. "Maximum Likelihood Localization of Multiple Sources by Alternating Projection". *IEEE Trans. on ASSP*, ASSP-36:1553–1560, Oct. 1988.

[142] M.D. Zoltowski, G.M. Kautz, and S.D. Silverstein. "Beamspace Root-MUSIC". *IEEE Trans. on SP*, 41:344–364, Jan. 1993.